Université de Montréal

Oxygenation-Sensitive Cardiovascular Magnetic Resonance Imaging (OS-CMR):
Potential Confounding Factors in use of OS-CMR

par
Gobinath Nadeshalingam

Sciences biomédicale 2e.
Médecine

Mémoire présenté à la Faculté de Médecine
en vue de l'obtention du grade de M.Sc.
en Science biomédicale
option Recherche clinique

Décembre, 2015

Université de Montréal

Faculté de Médecine

Ca mémoire intitule:

Oxygenation-Sensitive Cardiovascular Magnetic Resonance Imaging (OS-CMR):
Potential Confounding Factors in use of OS-CMR

Présentée par

Gobinath Nadeshalingam

A été évalué par un jury composé des personnes suivantes :

Dr. Michel White	Président rapporteur
Dr. Matthias Friedrich	Directeur de recherche
Dr. Jonathan Afilalo	Membre du jury

Resume:

La résonance magnétique cardiovasculaire sensible à l'oxygénation (OS-CMR) est devenue une modalité d'imagerie diagnostique pour la surveillance de changements dans l'oxygénation du myocarde. Cette technique offre un grand potentiel en tant qu'outil diagnostic primaire pour les maladies cardiovasculaires, en particulier la détection non-invasive d'ischémie. Par contre, il existe plusieurs facteurs potentiellement confondants de cette technique, quelques-uns d'ordre méthodologique comme les paramètres de séquençage et d'autres de nature physiologiques qui sont peut compris. En raison des effets causés par le contenu tissulaire d'eau, l'état d'hydratation peut avoir un impact sur l'intensité du signal. Ceci est un des aspects physiologiques en particulier dont nous voulions quantifier l'effet confondant par la manipulation de l'état d'hydratation chez des humains et l'observation des changements de l'intensité du signal dans des images OS-CMR.

Méthodes:
In vitro: Du sang artériel et veineux de huit porcs a été utilisé pour évaluer la dilution en série du sang et son effet correspondant sur l'intensité du signal de la séquence OS. *In vivo*: Vingt-deux volontaires en santé ont subi OS-CMR. Les concentrations d'hémoglobine (Hb) ont été mesurées au niveau de base et immédiatement après une l'infusion cristalloïde rapide de 1000 mL de solution Lactate Ringer's (LRS). Les images OS-CMR ont été prises dans une vue mid-ventriculaire court axe. L'intensité du signal myocardique a été mesurée durant une rétention respiratoire volontaire maximale, suite à une période d'hyperventilation de 60 secondes. Les changements dans l'intensité du signal entre le début et la fin de la rétention de la respiration ont été exprimés relativement au niveau de base (% de changement).

Résultats:
L'infusion a résulté en une diminution significative de l'Hb mesurée (142.5±3.3 vs. 128.8±3.3 g/L; $p<0.001$), alors que l'IS a augmenté de 3.2±1.2% entre les images du niveau de base en normo- et hypervolémie ($p<0.05$). L'IS d'hyperventilation ainsi que les changements d'IS induits par l'apnée ont été attenués après hémodilution ($p<0.05$). L'évaluation quantitative T2* a démontré une corrélation négative entre le temps de T2* et la concentration d'hémoglobine ($r=-0.46$, $p<0.005$).

Conclusions:
Il existe plusieurs éléments confondants de la technique OS-CMR qui requièrent de l'attention et de l'optimisation pour une future implémentation clinique à grande échelle. Le statut d'hydratation en particulier pourrait être un élément confondant dans l'imagerie OS-CMR. L'hypervolémie mène à une augmentation en IS au niveau de base et atténue la réponse IS durant des manoeuvres de respiration vasoactives. Cette atténuation de l'intensité du signal devrait être tenue en compte et corrigée dans l'évaluation clinique d'images OS-CMR.

Mots-cles:
La résonance magnétique cardiovasculaire sensible à l'oxygénation; éléments confondants; l'hémoglobine; hémodilution

Abstract:

Background:
Oxygenation-sensitive cardiovascular magnetic resonance (OS-CMR) has become a feasible diagnostic imaging modality for monitoring changes of myocardial oxygenation. This technique has great potential for use as a primary diagnostic tool for cardiovascular disease, particularly non-invasive detection of ischemia. Yet, there are several potential confounding factors of this technique, some methodological, such as sequence parameters and others are physiological and not well understood. Due to T2 effects caused by tissue water content, the hydration status may impact signal intensity. This is one physiological aspect in particular that we aimed at quantifying the confounding effect by manipulating hydration status in humans and observing signal intensity (SI) changes in OS-CMR images.

Methods:
In vitro: Arterial and venous blood from eight swine were used to assess serial dilution of blood and it corresponding effect on OS sequence signal intensity. *In vivo:* Twenty-two healthy volunteers underwent OS-CMR. Hemoglobin (Hb) concentrations were measured at baseline and immediately following rapid crystalloid infusion of 1,000ml of Lactated Ringer's solution (LRS). OS-CMR images were acquired in a mid-ventricular short axis view. Myocardial SI was measured during a maximal voluntary breath-hold, after a 60-second period of hyperventilation. SI changes were expressed relative to baseline (% change).

Results:
The infusion resulted in a significant decrease in measured Hb (142.5±3.3 vs. 128.8±3.3 g/L; $p<0.001$), while SI increased by 3.2±1.2% between baseline images at normo- and hypervolemia ($p<0.05$). Both hyperventilation SI and the SI changes induced by apnea were attenuated after hemodilution ($p<0.05$). Quantitative assessment showed a negative correlation between T2* and hemoglobin concentration ($r=-0.46$, $p<0.005$).

Conclusions:
There are several confounders to the OS-CMR technique that require attention and optimization for future larger scale clinical implementation. The hydration status in particular may be a confounder in OS-CMR imaging. Hypervolemia leads to an increase in SI at baseline and attenuates the SI response during vasoactive breathing maneuvers. This attenuation in signal intensity would need to be accounted for and corrected in clinical assessment of OS-CMR images.

Keywords:
Oxygenation-sensitive cardiovascular magnetic resonance; confounders; hemoglobin; hemodilution; breathing-maneuvers

Table of Contents:

List of Tables:

List of Figures:

List of Abbreviations:

CVD	cardiovascular disease
CAD	coronary artery disease
MRI	magnetic resonance imaging
rf	radio-frequency
TE	echo time
TR	repetition time
SWI	susceptibility-weighted imaging
BOLD	blood oxygen level dependent
OS-CMR	oxygenation-sensitive cardiovascular magnetic resonance
SI	signal intensity
SSFP	steady-state free precession
bSSFP	balanced steady-state free precession
HCT	hematocrit
Hb	hemoglobin
HV	hyperventilation
BH	breath-hold
HVBH	hyperventilation breath-hold

1.0 Background

Cardiovascular disease (CVD) remains today as the number one cause of death globally. Approximately 17.5 million deaths in 2012 were due to CVD. More specifically, an estimated 7.4 million of the total death due to CVD were caused by coronary artery disease (CAD)[1]. It is projected that death due to CVD will increase by 35% by the year 2030, and is projected to remain as the leading cause of death globally.

In the United States, costs related to cardiovascular disease were an estimated $475 billion in the year 2009. Interestingly, medical imaging for cardiovascular disease costs approximately $100 billion per year in the US. The growing burden of cardiovascular disease is evident as 29% of all imaging work is attributed to cardiovascular imaging[2]. The importance of imaging is two-fold: (1) it allows for the non-invasive assessment and diagnosis of disease severity, and (2) risk stratification of patients to guide treatment while also implementing imaging as a gatekeeper to invasive interventions. Currently, the most widely used imaging modalities are divided into functional imaging and anatomical imaging. The former allows for assessment of disease severity and consequences related to obstructive coronary disease, while the latter allows for the non-invasive visualization of the coronary tree[3].

2.0 Introduction to MRI

A MRI system is comprised of three main electromagnetic components: a set of main magnet coils, three gradient coils and a radio-frequency transmitter coil. The main magnet coils generate a strong, constant magnetic field denoted as B_0. B_0 is measured in units of Tesla (T), where 1 Tesla is equal to approximately 20,000 times the earth's magnetic field. A

coordinate reference system composed of three orthogonal axes (x, y, and z) is used to distinguish the magnetic field direction. The z-axis is by default chosen to be parallel to the direction of the main magnetic field, B_0[4].

The three gradient coils mounted inside the system can be rapidly switched on and off to generate a gradient magnetic field along the same direction as B_0 with varying strength along the aforementioned three axes (x, y, or z) corresponding to which gradient coil is activated. Essentially, the gradient magnetic field is superimposed on the B_0 field, yet its strength increases/decreases along the direction of the applied gradient field. Figure 1 shows the positioning of the three gradient coils within the MRI system and a visualization of the magnetic field generated by these gradient coils. The steepness of the slope of the gradient reflects the strength of the gradient magnetic field, measured in millitesla per metre (mT/m).

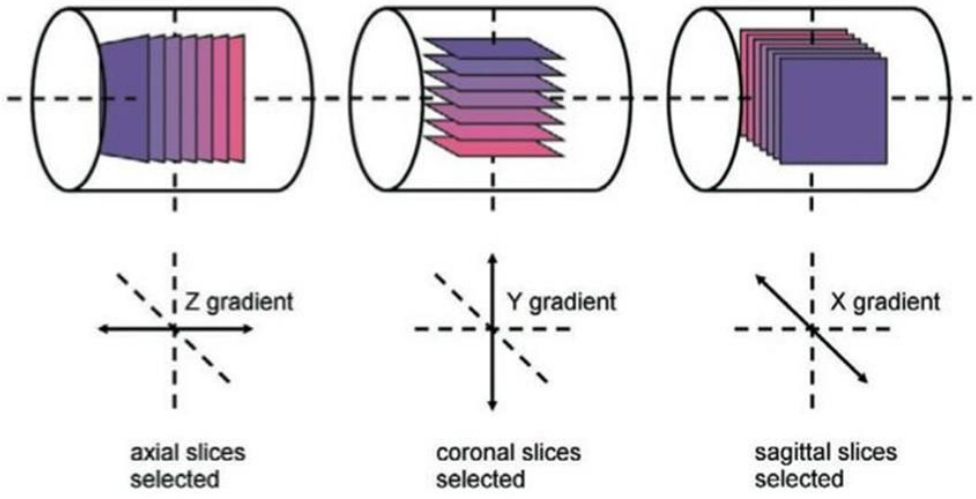

Figure 1: Visual representation of axial, coronal and sagittal slices, with dark purple color representing lower frequencies and pink representing higher frequencies[5].

The last electromagnetic component, the radiofrequency (rf) transmitter coil generates the rf magnetic field, often known as the B_1 field. The rf field generates a field that

oscillates at a specific frequency determined by the field strength of the main magnet. The rf magnetic field is used in a pulsatile manner to elicit excitation in protons causing their resonating magnetic field vector to be flipped along the orthogonal axes. As the magnetic field vector begins to relax and return to its equilibrium position the rf receiving coil in turn detects this relaxation to generate signals that create a MR image[5].

2.1 MR Signal Generation

The key to the generation of MR signals is the hydrogen nuclei, consisting of a single proton and electron. Hydrogen nuclei (protons) exhibit a phenomenon known as magnetic moment generated by an intrinsic property known as nuclear spin, giving the proton a small magnetic field with direction. Generally, these magnetic moments are randomly oriented in all directions, but when placed in the presence of an external magnetic field (like one generated by an MR system) these magnetic moments (spins) orient either parallel or anti-parallel with the B_0 field. An equilibrium state is quickly established where the excess magnetic moments aligning parallel with the B_0 field (a few per million) as it is energetically favorable and create a net magnetization vector (NMV) (a net magnetic field) in the z-axis direction (and B_0) (Figure 2). This net magnetization (M) at equilibrium is typically denoted as M_0[4].

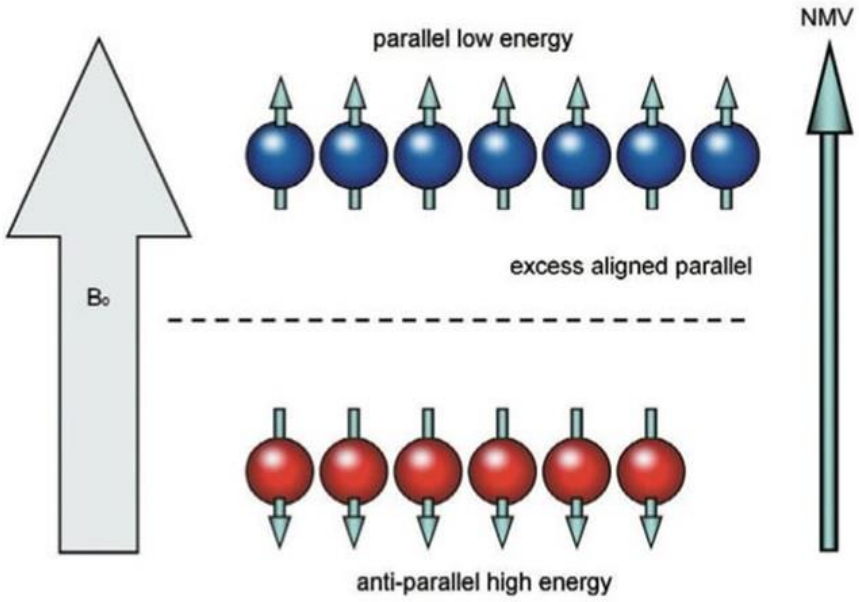

Figure 2: Illustration of net magnetization vector (NMV) formed from slight excess of protons aligned parallel (blue) to main magnetic field (B_0) as opposed to anti-parallel (red)[5].

The rf magnetic field is applied as a pulse at a specific frequency, known as the Larmor frequency (ω_0), to deliver energy to the population of protons at equilibrium. The Larmor frequency is determined by the Larmor equation:

$$\omega_0 = \gamma \times B_0$$

The constant γ is known as the gyromagnetic ratio with a value of 42.6 MHz/Tesla for the proton. The Larmor frequency, ω_0, is proportional to the main magnet field strength, B_0. Thus, for a 3 Tesla (3T) MR system the Larmor frequency is approximately 127.8 MHz. The Larmor frequency is also known as the resonant frequency, as this is the frequency at which protons within the MR system will absorb energy.

The rf pulse is delivered at right angles to B_0 and z-axis at the Larmor frequency causing the net magnetization M_0 to be shifted from the z-axis into the x-y plane. The "excited" protons will now spin around the z-axis in a spiral pattern at a frequency known as the precession frequency (also equal to the Larmor frequency). The amount of time the rf

pulse is switched on will determine how far the net magnetization will be shifted, this is known as the flip angle. Once the net magnetization has been shifted by a prescribed angle (α) the net magnetization can be divided into two component vectors. The first component is along the z-axis, known as the longitudinal component, and the second is within the planes of the x and y axes, known as the x-y or transverse component. Different rf pulses at different prescribed angles is demonstrated in Figure 3. A 90° rf pulse essentially causes the net magnetization to be completely shifted from the z-axis (longitudinal component) to the x-y plane (transverse component). A 90° rf pulse is also known as a saturation pulse for this reason, as it leaves no longitudinal component immediately after the pulse, all of the net magnetization is shifted to the transverse component.

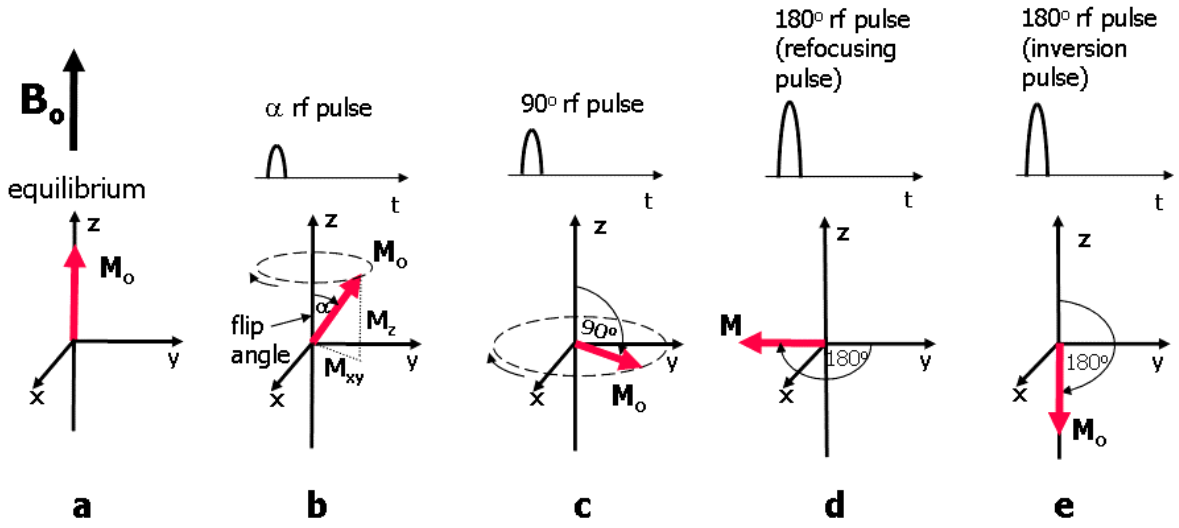

Figure 3: Illustration of differing states of magnetization: **a)** equilibrium state in which net magnetization (M_0) is aligned with the B_0 field along the z-axis; **b)** an rf pulse applied resulting in a flip angle α (less than 90°) causing net magnetization to be shifted from longitudinal (z-axis) at equilibrium state; **c)** application of saturation rf pulse, resulting in 90° flip angle and complete shifting of M_0 from longitudinal to transverse magnetization[4].

Radiofrequency excitation pulses with flip angles lower than 90° are also employed commonly allowing only a portion of the net magnetization to move from the longitudinal to

the transverse component. The major advantage of using a lower flip angle rf pulse is that it allows for a subsequent pulse to be applied close to the first pulse, as some of the magnetization still remains in the longitudinal component and can be shifted to the transverse component.

Ideally, all protons once excited by a saturation rf pulse will precess and continue precession at the Larmor frequency before slowly spinning back towards the z-axis and equilibrium. are inhomogeneities within the magnetic field and MR environment that cause some protons to lose their ideal Larmor precession frequency and rotate/spin slightly slower or faster than other surrounding protons resulting in dephasing or loss of coherence, and ultimately rapid degeneration of signal. Particularly in T2 sequences, where the transverse relaxation vector is of importance, this loss of coherence can be overcome by applying a 180° re-focusing pulse following the 90° saturation pulse to rotate the net magnetization through 180°, which results in re-focusing of the spins and coherence.

2.2 MR Signal Characteristics

Following excitation by rf pulse, protons immediately begin to relax and return to a state of equilibrium in which the net magnetization vector returns to the longitudinal (z) axis. The relaxation process can be separated into two components, longitudinal (z) and transverse (xy) relaxation. Longitudinal relaxation, or recovery of the magnetization along the z-axis is commonly referred to as T1 relaxation. Transverse relaxation on the other hand refers to the decay of the x-y component of net magnetization as it rotates about the z-axis and consequently the decay of the MR signal. Transverse and longitudinal relaxation occurs simultaneously.

2.2.1 T1 Relaxation

The T1 relaxation process is exponential and refers to the recovery of magnetization along the z-axis following a rf excitation pulse. T1 relaxation has a time constant known as T1 time, which occurs along the exponential recovery curve. The T1 time constant is a point along the exponential recovery curve when 63% of the original magnetization along the z-axis at equilibrium has recovered[4]. Figure 4 shows an example of the exponential T1 relaxation curve following a 90° rf pulse (saturation pulse). When a saturation pulse is applied, the net magnetization is immediately switched from z-axis (at equilibrium) to the xy (transverse) component, thus the magnetization for the z component is zero. The recovery of the magnetization for the z-component is rapid initially but slows as it approaches equilibrium. The recovery of the net magnetization along the z-axis following a saturation pulse is often appropriately known as saturation recovery. A short T1 time indicates faster recovery to equilibrium following an excitation pulse. The T1 time constant highlights important information about the characteristics of the tissues being imaged[5].

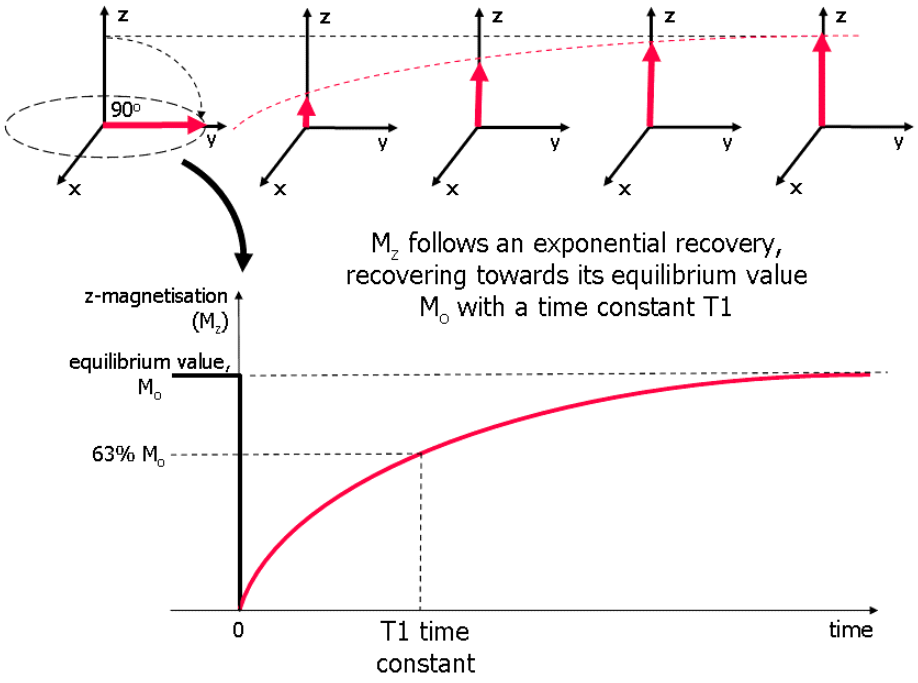

Figure 4: Exponential T1 recovery curve, illustrating the recovery of net magnetization along the z-axis following application of 90° saturation rf pulse[4].

2.2.3 T2 Relaxation

T2 relaxation or transverse relaxation is also an exponential process but unlike T1, which is an exponential recovery, T2 is an exponential decay of magnetization for the xy-plane. The T2 time constant is a point along the exponential decay curve at which the magnetization has decayed to 37% of the amount immediately following the 90° rf pulse. This is more easily understood when remembering that net magnetization is the sum of individual magnetic spins of a population of protons. Immediately following the rf pulse the population of protons have their magnetization flipped into the xy plane and they rotate (precess) together in a coherent manner in phase. As they rotate, each magnetic spin points in the same direction, as their precession frequencies are identical, thus they point in the

same direction in the xy plane. At any given instant, the angle of the magnetic spin is known as the phase angle. Magnetic spins having similar phase angles are referred to as being "in phase". Ideally, all spins would rotate with the same frequency as they approach equilibrium, thus resulting in a smooth exponential decay curve. In reality, following the rf pulse, the phase angles do not stay same, instead they begin to spread out, lose coherence and are referred to as being "out of phase". The net magnetization, which is the sum of the individual magnetic moments, is thus reduced resulting in the rapid decay of signal. As the protons precess in the xy-plane, they rotate around the z-axis as they approach equilibrium, thus the T2 relaxation curve is an oscillating exponential decay curve, and the process of decay is known as free induction decay (FID) (Figure 5). There are two major contributors to loss of coherence and decay of signal in T2 relaxation, which will be briefly discussed here.

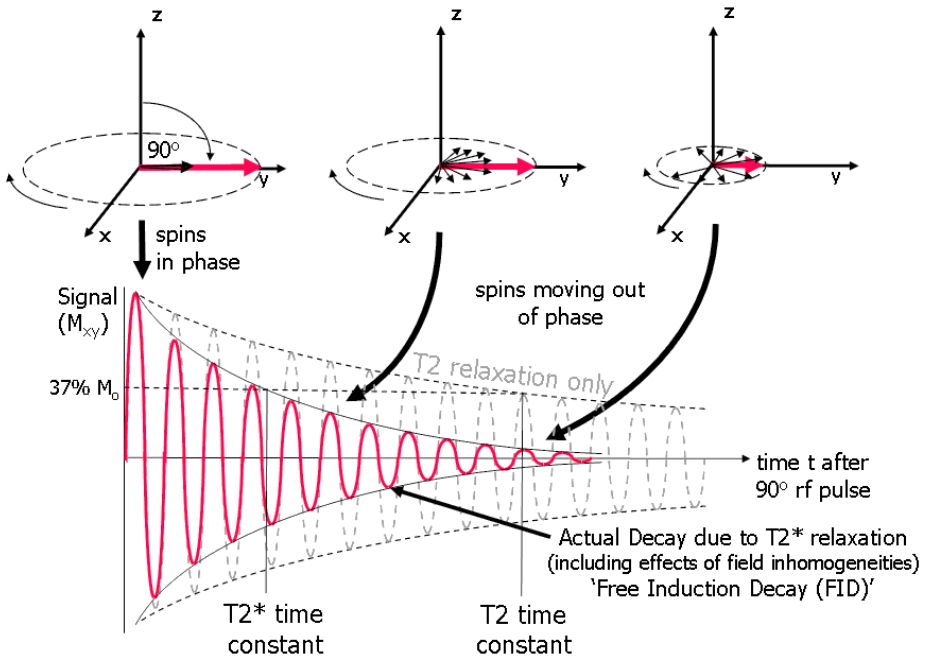

Figure 5: T2 and T2* relaxation following 90° saturation rf pulse, illustrated with T2 and T2* exponential decay curves[4].

The first cause of loss in coherence is due to the fact that although the population of protons will initially precess at the same frequency and be in phase, the magnetic spin of one atom can affect neighboring atoms. Due to the fact that protons are constituents of varying types of atoms, over time the phase angles of different protons will begin to differ in a random fashion. The net effect is the Larmor frequency of protons will begin to differ, ultimately causing loss of net magnetization in the xy-plane. This factor of the spin of one proton affecting neighboring protons is known as spin-spin interactions. Spin-spin interactions are of a random nature, thus the dephasing as a result of spin-spin interactions are not reversible[4].

The second contributor to loss of coherence is due to inhomogeneities in the applied B_0 magnetic field. Local variations along the magnetic field will cause the Larmor frequency to vary between different locations, thus resulting in loss of coherence or dephasing. Protons at different locations will precess at different frequencies following excitation by rf pulse and therefore cause a deviation from the ideal T2 relaxation curve in the absence of field inhomogeneities. Unlike spin-spin interactions, inhomogeneities are fixed and therefore dephasing due to this factor is potentially reversible. The combination of T2 relaxation, as a result of spin-spin interaction, and decay due to magnetic field inhomogeneities is known as T2* relaxation. T2* relaxation determines the actual rate of FID and is also an exponential decay process with a time constant T2*, determined in the same fashion as the T2 time constant.

2.2.4 Significance of T1 and T2 Values

The T1 and T2 values obtained can shed important information about the tissue being imaged, in addition the unique properties of T1 and T2 imaging can be exploited for creating protocols for imaging specific diseases and disease processes.

As mentioned in Section 2.2.1 T1 Relaxation, T1 imaging involves measuring T1 relaxation rate or time and the recovery of magnetization along the z-axis. This relaxation occurs when protons that have absorbed energy from the rf pulse release this energy to return to an equilibrium state. Thus, the rate at which energy is released by the excited protons is related to the relaxation rate. The tumbling rate, or the rate of molecular motion, of various molecules and macromolecules helps to determine whether energy exchange between neighbouring molecules is favourable. When the tumbling rate of a molecule is close to the Larmor frequency, energy exchange is most favourable, resulting in rapid relaxation or short T1 relaxation time[4]. T1 contrast images are generated by setting repetition time (TR) to be less than the total relaxation time of tissues. Thus, when the second rf pulse is applied, tissues that have recovered faster will have a large longitudinal component and therefore also a larger transverse component upon application of the second rf pulse. Fat, for example, loses transverse energy rapidly and has more rapid longitudinal recovery than water, therefore in T1 images fat has a large transverse component leading to high signal and consequently appearing bright on T1 contrast images. Water on the other hand, has a lower transverse component upon repeated rf pulse application, leading to lower signal and appearing darker on T1 contrast images. Contrast between fat and water can be improved by choosing an optimal TR so that the difference in the recovery of longitudinal component is the greatest[5]. Figure 6 demonstrates this concept, as can be seen, if TR is too long then both

fat and water will have fully recovered to B_0 not allowing for any delineation between tissue types.

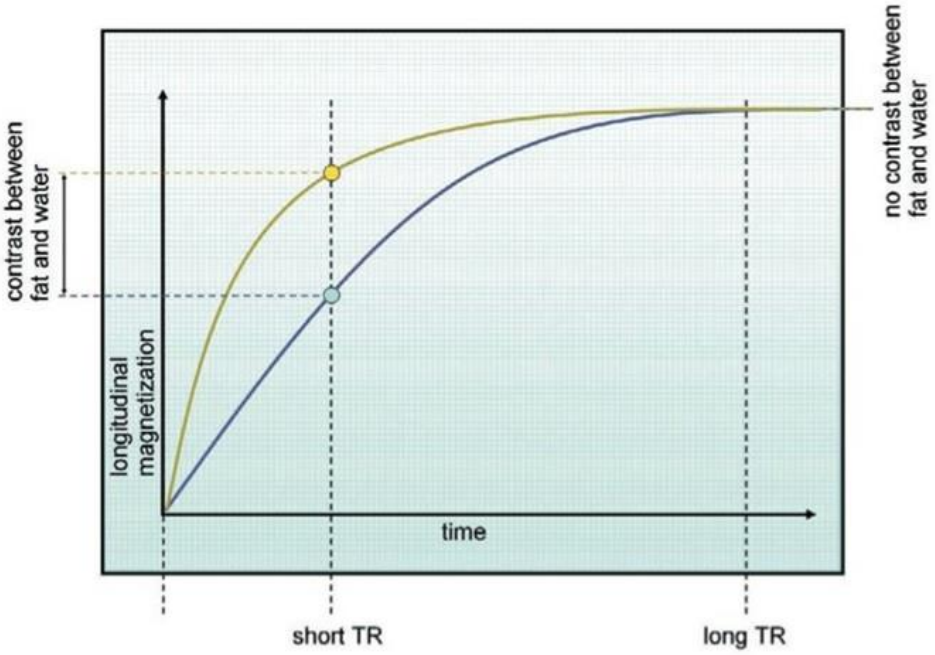

Figure 6: T1 difference between fat and water and illustration of how TR can be manipulated to maximize contrast between different tissues with varying fat and water content[5].

T2 relaxation rate is related to the amount of spin-spin interaction that occurs between molecules. When molecules are small, far apart and moving rapidly, such as free water, spin-spin interaction occurs less frequently and thus the T2 relaxation rate is slow, or T2 time is high[4]. T2 contrast is dependent on echo time (TE), which determines the amount of time allowed for decay of transverse magnetization before the signal is received. As discussed previously, due to low frequency of spin-spin interactions amongst water molecules, transverse magnetization decays slower and water has a larger signal, therefore appearing brighter on T2 images. On the other hand, decay of transverse magnetization is rapid in fat and thus fat appears dark on T2 images (Figure 7).

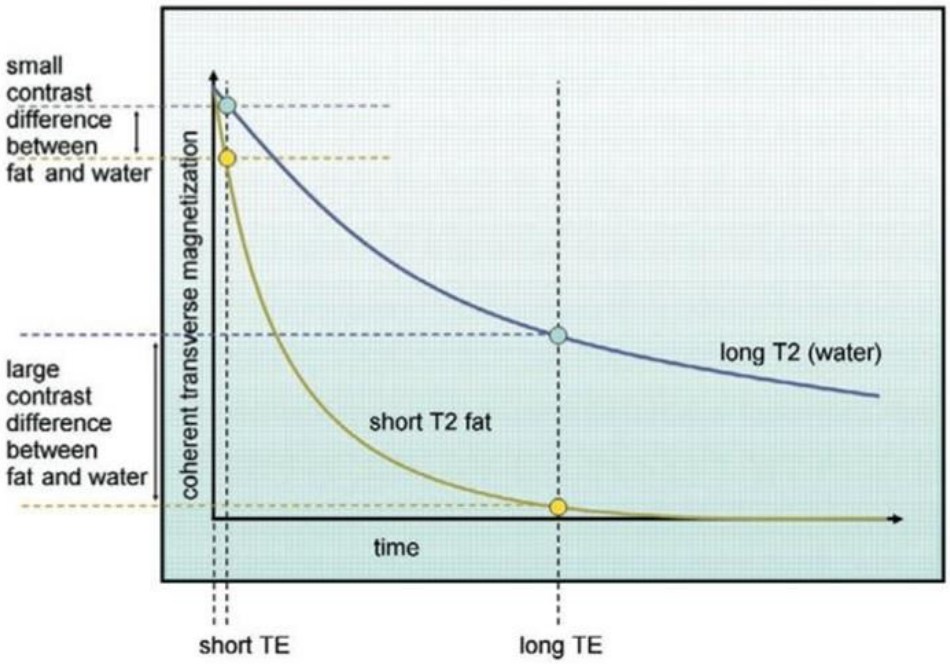

Figure 7: T2 differences between fat and water and illustration of how TE can be manipulated to maximize contrast between fat and water[5].

3.0 T2*, Susceptibility-Weighted Imaging (SWI), and BOLD/Oxygenation-Sensitive MR

3.1 Origins of BOLD-sensitive imaging

Ogawa et al.[6] conducted a study on mice brains using high magnetic fields (7T and 8.4T). The study was driven by the understanding that although MRI was quite good at distinguishing brain anatomy, it was no sensitive enough to detect normal metabolic changes in order to assess physiological events. Building on a previous study that presented the ability to measure blood flow using MR at 1.5T[7]; Ogawa et al., hypothesized that this technique could be exploited to understand brain physiology and metabolic activity since the latter is correlated with oxygen consumption and thus blood flow. The mice were ventilated to breathing various concentrations of oxygen, varying from anoxia to 100% oxygen. The images of the brain were first acquired when the animal was breathing 100% oxygen using

a gradient echo sequence. It was found that certain anatomical features were well defined but overall the contrast was quite poor. Interestingly, when the oxygen content in the breathing gas was reduced to 20%, there was a striking difference in the contrast, as many dark lines appeared within the image. It was also found that this change was reversible and the dark lines disappeared when oxygen content was increased. Using fixed slices of the brain and microscopy, and comparing with the dark lines produced in the images, it was clear that these lines were blood vessels. One of significant findings of this study was the conclusion that the contrast was generated by magnetic susceptibility due paramagnetic deoxyhemoglobin. This was deduced from the fact that when the anesthetized mice were sacrificed using carbon monoxide (which when bound to hemoglobin produced diamagnetic carboxyhemoglobin), most of the contrast seen from breathing 20% oxygen disappeared. On the other hand, when the animal was left under anoxic conditions, the contrast was very high. Another striking difference was seen when comparing spin echo and gradient echo sequences. It was noted that the contrast produced by the gradient echo was not present when using a spin echo sequence. This was further tested by use of concentric double tubes, where blood was placed in the center tube and saline in the outer. Both oxygenated and deoxygenated blood were examined using both sequences. As seen in (Figure 8), when examining oxygenated blood there was very little difference when comparing sequences. On the other hand, a noticeable difference was seen in the deoxygenated blood when comparing both sequences.

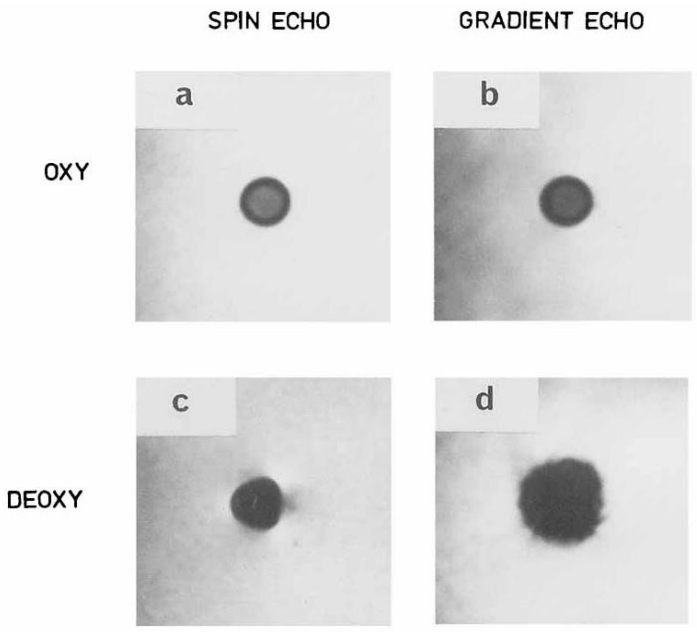

Figure 8: Oxygenated and deoxygenated blood compared using spin-echo and gradient-echo sequences[6].

Ogawa further built on this research in a subsequent study by directly modifying blood oxygen levels and observing the effect on oxygenation-sensitive MRI[8]. The term BOLD (blood oxygenation level-dependent) contrast was coined for the technique of assessing oxygenation using MRI. It was determined that BOLD contrast was ultimately a result of the balance of 2 factors: oxygen supply (blood flow) and oxygen extraction by tissues (metabolism). The study found that there was a blood flow-dependent loss in BOLD contrast, as observed when animals were switched from breathing 100% oxygen to 10% CO_2/90% O_2. It was observed that blood CO_2 increased from 50 to 80 mmHg, which would subsequently cause an increase in blood flow and thus a greater supply of oxygen to the brain. Thus the increased flow, in the absence of increased metabolic activity led to a decrease in deoxyhemoglobin concentration and thus loss of contrast. In addition, the group assessed changes in contrast due to insulin-induced hypoglycemia. It was found that following insulin

injection, BOLD contrast was greatly reduced. Although there was a slight increase in blood flow due to hypoglycemia, it was concluded that the loss of contrast could not be entirely due to flow but also due to decreased metabolism. The study provided the groundwork for the idea that BOLD imaging could be used for in vivo brain mapping to detect local changes in metabolic activity by tracking changes in blood oxygenation due to increased or decreased oxygen consumption.

3.2 Oxygenation-sensitive cardiac imaging (OS-CMR)

3.2.1 Pre-clinical studies

One of the first studies to translate the research of Ogawa to cardiac imaging was done by Atalay et al. in 1993[9]. In the study, four New Zealand white rabbits were sacrificed and the hearts were harvested. The hearts were perfused using varying oxygen saturation perfusate (bovine blood) with a Langendorff apparatus. The goal was to use high-field strength (4.7T) MR and susceptibility-dependent imaging to determine if myocardial oxygenation could be measured. Five to nine images were acquired for each heart using varying range of hemoglobin concentrations, with the first and last images being taken using perfusate that was fully saturated. The results were very promising, as the group observed that signal intensity (SI) varied linearly with perfusate oxygenation level, leading to the conclusion that the difference between signal intensity was due to paramagnetic effects of deoxyhemoglobin.

Wendland et al., also in 1993[10], used a rat model to show that apnea or varying lengths resulted in changes in susceptibility-dependent MR myocardial signal intensity. The group performed 45 and 90 second periods of apnea by shutting off the ventilator after 6 or 7

images had been obtained and then continued imaging during apnea. Blood samples were obtained prior to and following apnea and analyzed using a blood gas analyzer. There was a significant decrease in myocardial signal intensity from baseline associated with the two different periods of apnea. Likewise, there was a significant decrease in pO_2 and O_2 saturation associated with apnea. The study concluded that it was feasible to use MR to measure changes in myocardial SI associated with apnea and consequently perturbations in local myocardial deoxyhemoglobin concentrations.

Following these two animal studies, many questions still remained about the potential confounding factors of blood flow and volume differences in varying vessels of the heart to influence SI in oxygenation-sensitive imaging. Li et al., attempted to tackle these issues in a study using thirteen healthy human volunteers[11]. The purpose of the study was to assess changes in myocardial signal intensity due to two pharmacological agents: dipyridamole and dobutamine. These drugs were chosen as both cause increase in myocardial blood flow but utilize different mechanisms to do so. Dipyridamole is a potent coronary vasodilator, leading to a 3- to 4-fold increase in flow but causes very little change to myocardial oxygen consumption[12]. Thus, with no change in oxygen demand, but an increase in supply, venous blood oxygenation is generally increased. On the other hand, dobutamine is a potent $beta_1$-agonist leading to an increase in myocardial oxygen consumption, and thus consequently leading to an increased oxygen demand and myocardial perfusion. In the case of dobutamine, venous blood oxygenation does not change as the increase in oxygen consumption is balanced with the increase in oxygen supply. The imaging was done using a 1.5T MRI system and a gradient-echo sequence. The group found that dipyridamole induced blood flow velocity to increase by 124±27% and T2* (SI) increase of

46±22%. Contrastingly, dobutamine caused a 41±25% increase in coronary flow, and correspondingly no increase in SI (-5±19%). As hypothesized, the increase in blood flow due to dipyridamole, with no resultant increase in oxygen demand, resulted in increased concentration of oxyhemoglobin to deoxyhemoglobin, thereby reducing susceptibility effects and leading to an increase T2*. Similarly, the injection of dobutamine led to an increase in oxygen demand, but with resulting balanced oxygen supply, there was no change in concentration of deoxyhemoglobin, and thus no change in T2*. This study was of major importance as it helped to exclude various factors such as blood volume and velocity as potential confounder to oxygenation-sensitive imaging and paved the way for future studies using the technique.

In 2005, Shea et al., conducted a study to assess the feasibility of using a T2-prepared steady-state free precession BOLD imaging sequence for detecting SI changes in a stenosis model[13]. The group argued for the use of a T2 sequence as opposed to the traditionally used T2*-weighted sequence highlighting that T2* sequences were much more susceptible to local field inhomogeneities and that T2-weighted sequences were less susceptible to motion artifact and produced better signal-to-noise ratios.

Building on the findings of Li et al., Vöhringer et al., conducted a study to assess feasibility of SSFP BOLD-CMR to accurately detect changes of myocardial oxygenation in vivo[14]. The study utilized a canine model to assess the hypothesis using selective intracoronary vasodilation. A 1.5T MRI system was used and single mid-ventricular short-axis slice was used for images. The sequence used for imaging was a T2*-sensitive cine SSFP (TR/TE: 5.8ms/2.9ms, flip angle = 90°). Acetylcholine was infused into the left circumflex artery (LCX) at three increasing doses: 0.1 μg/min (Ach1), 1 μg/min (Ach2), and 10 μg/min

(Ach3). Similarly, adenosine was infused at 3 increasing rates: 30 μg/min (Ade1), 150 μg/min (Ade2), and 300 μg/min (Ade3). The imaging protocol was as follows: BL1, Ach1-3, BL2, Ade1-3, and BL3 (where BL was baseline). The study observed a significant increase in LCX blood flow associated with drug-induced vasodilation in addition to no significant change in flanking repeated baseline measurements. Blood flow increase was dose-dependent, but was associated with progressively smaller increases in coronary sinus oxygen saturation (SvO_2). Interestingly, the group found a correlation ($r^2 = 0.84$, $p<0.001$) and exponential relationship when comparing SvO_2 and LCX flow, with SvO_2 approaching a horizontal asymptote around 87% when mean arterial oxygen saturation reached 96.7% (Figure 9, left). Most importantly, it was observed that there was a linear relationship between SvO_2 and SI generated from oxygenation-sensitive CMR (Figure 9, right). The study was one of the first to compare use of a T2*-sensitive SSFP BOLD sequence to compare changes in SI associated with intracoronary vasodilators. Interestingly, the group suggested the potential for use of this sequence for assessment of myocardial ischemia, by

extrapolating the linear correlation graph into ischemic range.

3.2.2 Clinical Studies

Wacker et al., completed one of the first studies assessing OS-CMR in a CAD patient population[15]. The study was composed of 16 healthy volunteers, with no previous history of cardiovascular disease, and 16 patients, with known single-vessel CAD with >70% stenosis on coronary angiogram. Imaging was completed using a 1.5T MRI system using a segmented gradient echo pulse sequence. Images were acquired at baseline and repeatedly following dipyridamole infusion every minute until heart rate returned to baseline level. In the volunteers, T2* SI increased significantly by 10±5% following dipyridamole infusion. However, in the patients, even under rest conditions, regions with reduced T2* SI could be identified, and corresponded with areas of wall motion abnormalities. Two of the patients from the study underwent PCTA and CABG, and were re-assessed following their respective

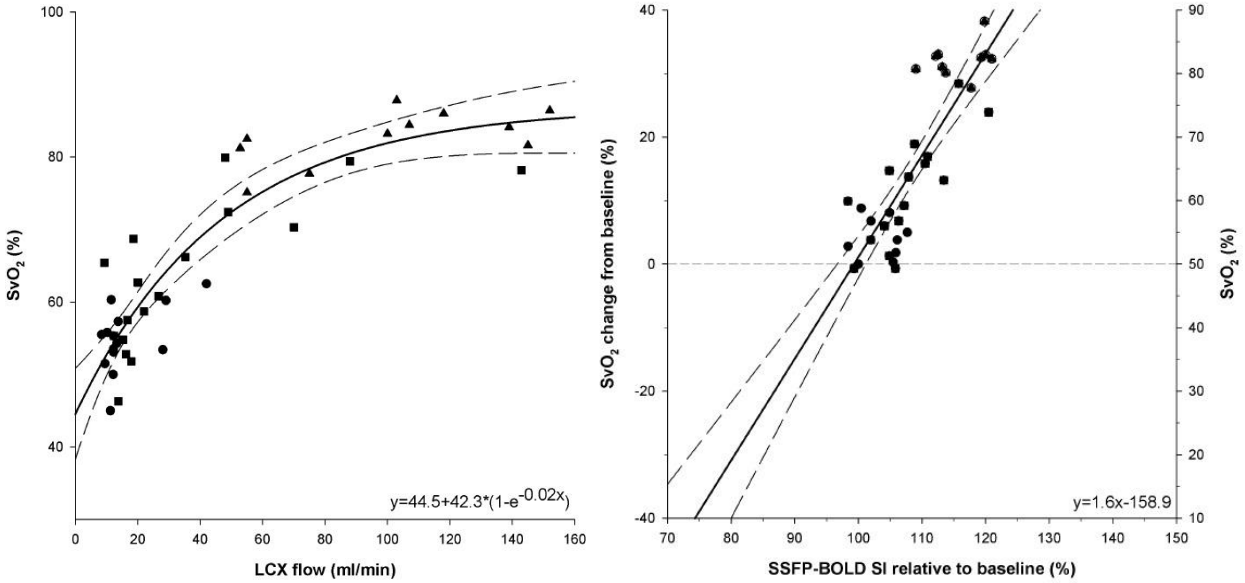

Figure 9: LEFT: Comparing coronary sinus oxygen saturation (SvO_2) and LCX (left coronary artery) blood flow; RIGHT: Linear correlation of SvO_2 and signal intensity generated by oxygenation-sensitive CMR[14].

procedures (10 weeks and 20 week, respectively). It was found that regions that previously

showed marked reductions in T2* compared with normal myocardium, were less pronounced following interventions.

In the same year (2003), Friedrich et al. conducted a study with 25 patients to compare stress-induced angina OS-CMR results with results generated by quantitative angiography and thallium single-photon emission computed tomography (SPECT)[16]. Imaging was completed using a 1.5T MRI system and a single-slice T2*-sensitive gradient-echo planar imaging pulse sequence for OS images. Quantitative angiography indicated that 23 of the 25 patients had coronary stenoses >50%, additionally 10 of these patients had stenoses >75% (severe). Oxygenation-sensitive CMR results showed a mean SI change of +0.94±0.67% for segments with no stenosis, +0.27±0.63% for segment associated with stenosis <50%, and +0.84±0.76% for segments related to stenosis of 50-75%. Most interestingly, segments associated with a stenosis >75% showed a significant mean change of -2.33±0.99%. The study identified an optimal cutoff value of 1.2% for SI change to delineate segments related with <75% or ≥75% stenosis. Using 1.2% as a cutoff value, OS-CMR displayed a sensitivity of 88% and specificity of 47%. Similar results were found when assessing SPECT data, although there was no significant correlation between the results from OS-CMR and SPECT. The group concluded that for the patient population studied, OS-CMR compared favorably with thallium SPECT, and given the fact that OS-CMR directly measures tissue oxygenation, it could have promise for clinical use.

Manka et al. built on previous research and conducted a patient study using a 3T MRI system to assess the ability of OS-CMR to detect stress-inducible myocardial ischemia[17]. The study was composed of forty-six patient with suspected or known CAD who underwent OS-CMR imaging prior to clinically-indicated coronary angiography. Quantitative coronary

angiography was used as the standard of reference and defined 3 types of segments: 1) normal segments (segments in patients with no CAD), 2) ischemic segments (supplied by coronary arteries with >50% stenosis), and 3) non-ischemic segments (supplied by coronary artery without significant stenosis in patients with significant CAD). At rest, ischemic segments of the myocardium showed much lower T2* than normal segments and non-ischemic segments (26.7±11.6 ms, 31.9±11.9 ms, and 31.2±12.2 ms, respectively). During adenosine-induced stress, T2* values increased significantly in normal segments (37.2±14.7 ms), but did not increase significantly in non-ischemic and ischemic segments when comparing rest and stress. The group also calculated global T2* values and found that in patients without significant CAD, T2* changed significantly between rest and stress (32.2±3.5 ms vs. 37.4±6.3 ms, respectively). Contrastingly, in patients with significant CAD, global T2* value showed no significant difference between rest and stress (30.3±5.3 ms vs. 30.7±5.5ms, respectively). The study concluded that it was feasible to use 3T OS-CMR to differentiate normal, ischemic and non-ischemic myocardial segments. Additionally, the study showed the ability of OS-CMR to non-invasively identify patients with significant CAD.

Another study conducted in the same year, Karamitsos et al., attempted to elucidate the interplay of ischemia, perfusion, and oxygenation in CAD using OS-CMR[18]. The study assessed twenty-two patients with CAD, defined as at least one stenosis >50% on quantitative coronary angiography (QCA). In addition, they study assessed ten healthy, age-matched volunteers. The patients and volunteers underwent OS-CMR using a 3T MRI system at rest and during adenosine-induced stress. The imaging was completed using a single mid-ventricular slice and a T2-prepared ECG-gated SSFP sequence (TR: 2.86ms, TE: 1.43ms; flip angle: 44°). Patients and volunteers also underwent a PET scan using oxygen-15-labeled

water, again at rest and stress. PET scans were used as a method to measure myocardial blood flow (MBF) and coronary flow reserve (CBF). Using QCA as the gold standard, cut-off values were established for both PET and OS-CMR. A cut-off value of stress MBF ≤2.45mL/min/g was determined for segments that were supplied by significantly stenosed vessels (79% sensitivity, 84% specificity). Similarly, for OS-CMR after stress, <3.74% change in SI defined segments supplied by stenosed vessels (sensitivity: 67%, specificity: 88%). The group also noted good agreement between the two techniques on a per-subject basis. The study found, in CAD patients, there was a dissociation in a significant proportion of myocardial segments between regional blood flow (perfusion) and oxygenation. It was noted that 40% of segments with impaired hyperemic blood flow, as assessed with PET, showed normal oxygenation at stress. Conversely, in 88% of segments where hyperemic blood flow was above the cut-off value, oxygenation was also normal. The significant contributions of this study was the notion that reduced blood flow and perfusion at stress within segments classified as having significant stenosis (using QCA), do not necessarily display reduced oxygenation. It also highlighted the potential for OS-CMR to play a gatekeeper role for invasive interventions by determining hemodynamic significance of stenosis by assessing changes in oxygenation. In 2012, the same research group, building on the previous results, conducted a study comparing the same OS-CMR sequence (T2-prepared SSFP) to first-pass perfusion images at rest and stress in sixty patients with suspected CAD[19]. All patients were scheduled for elective angiography as part of routine clinical care. Using QCA as a reference, it was found that 68% of patients had significant CAD. For identifying significant stenosis using OS-CMR it was noted that the technique displayed an accuracy of 86%, a sensitivity of 92% and a specificity of 72%. When using perfusion as the reference standard, OS-CMR

(using a cut-off value of 2.64% change in SI) displayed a diagnostic accuracy of 84%, sensitivity of 92% and specificity of 72% for identifying significant coronary stenosis. The group concluded once again that hypoperfusion may not necessarily indicate deoxygenation and cellular ischemia, noting that OS-CMR achieved favorable accuracy for identifying significance of CAD.

Walcher et al., also in 2012, aimed to validate BOLD-CMR by comparing it against the invasively measured gold-standard, fractional flow reserve (FFR)[20]. The study assessed thirty-six patients with angina pectoris and suspected CAD using a 1.5T system. For BOLD imaging, a T2-prepared SSFP sequence was utilized (TR: 2.6 ms; TE: 1.3 ms, flip angle: 90°), and images acquired in 3 short-axis slices (apical, midventricular, and basal). BOLD imaging protocol was completed both at rest and following adenosine-infusion. For FFR measurements, a value ≤0.80 during adenosine infusion was chosen as a cut-off value for identifying coronary stenoses causing ischemia. The group found that BOLD-CMR values and invasively-measured FFR values were highly correlated. It was found that BOLD-SI of myocardial segments supplied by coronary arteries with FFR≤0.80 were significantly lower than those segments supplied by arteries with FFR>0.80. It was concluded that BOLD-CMR could serve as an alternative to first-pass perfusion for the detection of hemodynamically significant CAD.

3.2.3 OS-CMR and Blood Gas Manipulation

For OS-CMR to have clinical potential it requires some mechanism of inducing cardiac stress, as seen in the various aforementioned clinical studies. The pharmacological stress agent most commonly used for CMR is adenosine. Karamitsos et al., conducted a study with

351 consecutive patients with suspected or known CAD[21]. There were no serious adverse events observed in this study, but in four patient the scan had to be stopped during adenosine at the subjects' request. Most striking was the occurrence of chest pain, breathlessness, and flushing, headache or dizziness which occurred in 57%, 45% and 43% of patients, respectively. This highlights the underlying issue that although adenosine is tolerated, in almost half of all patients that receive intravenous adenosine infusion, there is discomfort. In addition, in 2013, the U.S. Food and Drug Administration (FDA) released a safety announcement regarding the rare but serious risk of heart attack and death related to the use of adenosine and regadenoson[22]. This underscores the need for viable alternatives to pharmacological stress agents, such as adenosine, if possible.

Carbon dioxide is a potent vasodilator that has been examined in the brain, and more recently heart, to show that even small increases induced by breath-holding can increase cerebral and myocardial blood flow[23–26]. Guensch et al., showed this effect of increased myocardial blood flow using a swine model[27]. The authors utilized a T2*-weighted SSFP sequence and a 1.5T MRI system. The group induced 60-second breath-holds in nine anesthetized swine and acquired OS-CMR images throughout the breath-hold. Blood samples were taken immediately prior to and following the breath-hold and analyzed using a blood gas analyzer to assess changed in blood gases due the breath-hold. A strong linear correlation ($r=0.90$, $p=0.010$) between change in $paCO_2$ and change in myocardial SI was found. The study indicated the potential for CO_2 manipulation, such as breath-holding, to be used in combination with OS-CMR for diagnostic imaging.

Guensch et al., building on previous animal study, conducted a study with healthy human volunteers to assess the feasibility of using OS-CMR combined with breathing

maneuvers to elicit changes in myocardial blood flow and consequently myocardial signal intensity[28]. The study recruited eight healthy volunteers and six aquatic athletes to perform various breathing maneuvers. The eight volunteers performed a free maximal breath-hold and 2 sets of hyperventilation of 1 and 2 min each. The aquatic athletes performed a timed 60-second breath-hold and a maximal breath-hold. The identical imaging parameters were used. The study found that free maximal breath-holds resulted in a significant increase (8.2%) in myocardial SI, and conversely, hypoventilation by 120 seconds of hyperventilation led to a significant decrease (7.5%) in myocardial SI. The major contribution of this study was observed changes in myocardial SI due to hyperventilation, which could be observed using OS-CMR. The decrease in pCO_2 as a result of hyperventilation, lead to vasoconstriction, decrease in myocardial blood flow and consequently a drop in SI. This study highlighted the potential for combining hyperventilation and apnea to produce changes in myocardial signal intensity for clinical use of OS-CMR sequences, especially if the change produced by breathing maneuvers could be comparable to adenosine.

Most recently, Fischer et al., compared the vasodilatory potential of the aforementioned breathing maneuvers to adenosine using OS-CMR imaging[29]. The study recruited twenty healthy volunteers who underwent OS-CMR imaging using a 3T MRI system. A balanced steady-state free precession (bSSFP) sequence was used (TE/TR: 1.70/3.4 ms, flip angle: 35°). The volunteers performed a combined 60 second hyperventilation followed by maximal voluntary breath-hold maneuver. A single measurement was acquired prior to hyperventilation and imaging was acquired continuously during the breath-hold. In addition, the volunteers performed a maximal breath-hold (without hyperventilation). Lastly, the volunteers received adenosine infusion

(140µg/kg/min), where image acquisition took place immediately before and 3.5 minutes after beginning of the infusion. It was found that pharmacological vasodilation with adenosine resulted in an increase of 3.9±6.5% in myocardial SI. Contrastingly, hyperventilation produced a significant decrease (-10.6±7.8%) in SI, and the following maximal breath-hold produced an increase (14.8±6.6%) in SI. The maximal breath-hold without hyperventilation produced an increase in SI similar to that of adenosine (3.1±3.9%). The study concluded that combination of hyperventilation and maximal breath-hold produced a much larger change in myocardial oxygenation than standard dose of adenosine, as assessed by OS-CMR. This study is of major importance as it shows that breathing maneuvers could serve as a viable alternative to the use of adenosine. Breathing maneuvers not only produces a much larger change in signal intensity, but are safer, more efficient and less costly and thus may be a much better tool, when combined with OS-CMR, for assessing coronary vasomotor response. This study also assessed the tolerance of breathing maneuvers compared to adenosine infusion, using self-reported discomfort levels associated with both. It was found that breathing maneuvers were much better tolerated as no subject reported that the maneuvers were difficult or inconvenient.

4.0 Potential Confounders of OS-CMR

4.1 Artifacts

The homogeneity of the B_0 magnetic field is critical component in acquiring images without signal loss or artifact. The B_0 homogeneity of an empty magnet is very high, but this homogeneity is greatly reduced when a patient is inside the bore due to susceptibility. Magnetic susceptibility refers to the ability of an object placed in the magnetic field to

become magnetized itself. Depending on the type of material, air, water, and different biological tissues, this susceptibility can vary greatly. Additional magnetic fields produced by the objects themselves cause inhomogeneity in the B_0 field and result in susceptibility artifacts. Most importantly, variations causes by susceptibilities are proportional to field strength, therefore making susceptibility artifacts much more pronounced at 3T than 1.5T[30].

One of the major benefits of using a 3T system, increased signal-to-noise-ratio (SNR), also leads to increased artifact-to-noise-ratio (ANR). In regards to bSSFP sequences, they are sensitive to off-resonance effects, which often results in banding artifacts in the acquired image. Additionally, artifacts from pulsatile flow are also increased when using 3T[31]. Correction for artifacts and sequence optimization to minimize artifacts still remains a major limitation of 3T OS-CMR. Shimming techniques are often employed to correct for field inhomogeneities in the magnetic field.

4.1.1 Lung-heart interface susceptibility artifacts

Atalay et al. noted that significant magnetic field inhomogeneities were observed surrounding the myocardium at magnetic field strengths 1.5T and greater[32]. These artifacts were most frequent along inferoapical myocardial region. The group assessed (using an animal model) various sources for the origin of the artifact and concluded that the interface between the myocardium and the lungs was the primary cause of these artifacts. Additionally, the group acquired images post-euthanasia at three different TEs, and filled the chest cavity with aqueous $CuS0_4$ solution, in attempt to remove air in the chest cavity as a confounding factor in artifact generation. Figure 10a shows the image acquired with a TE of 4.7 ms, where the edges of the right and left lung can be seen generating triangular-shaped

artifacts. These artifacts became larger with increasing TE (Figure 10b and c). Finally, when the lung was resected the artifact in the myocardium was no longer observed (Figure 10d). The conclusion was reached that the large difference in magnetic susceptibility between air and tissue was the primary reason, as the artifact disappeared with lung resection.

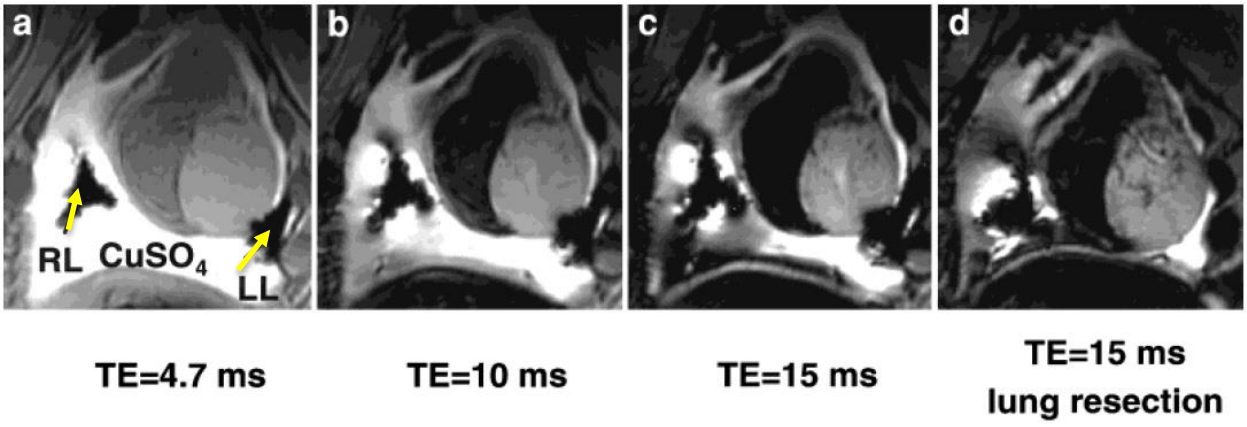

Figure 10: Post-euthanasia images with chest cavity filled with aqueous $CuS0_4$. Images **a-c** show the effect of varying TE on the image distortions, while **d** shows the effect of partially resecting the lungs on apical artifacts. RL: right lung; LL: left lung[32].

4.1.2 Metal implants

Metal implants, specifically ferromagnetic implants, are a contraindication for MR imaging in patients. Nijveldt et al., demonstrated that CMR at 3.0T was feasible in patients treated with stenting[33]. Although image quality was sufficient, quantitative assessment was less reliable than 1.5T due to dark band, flow and stent artifacts. The group concluded that further optimization of the sequences was necessary for clinical use[34].

Generally, the risks associated with ferromagnetic implants are migration, induction of an electrical current and heating, all of which are described by Levine et al. in "Safety of Magnetic Resonance Imaging in Patients with Cardiovascular Devices"[35]. Ferromagnetic objects experience an attractive force in the presence of a magnetic field, as a result, these

devices may be moved, rotated, dislodged, or accelerated toward the magnet. This migration of implanted devices has the potential to cause significant patient injury. During the course of an MR examination, rf pulses transmit energy to the body of the patient. Some metallic devices can act as an "antenna" causing concentration of rf energy and thus leading to excessive localized heating. Induction of electrical currents in implantable devices is possible due the use of gradient magnetic fields, which are rapidly turned on and off during image acquisition. Levine et al. found that although current-generation scanners may not directly excite cardiomyocytes, there is potential for induced currents to cause arrhythmias.

In addition to posing risk to the patient or the MR system, metallic implants may have a significant effect on the quality of images obtained. The most prevalent image artifact associated with metallic objects is loss of signal due to more rapid dephasing of spins. Thus, near metal objects there is loss of signal and black areas on the acquired image[36]. Although many implanted cardiac devices/objects are safe for imaging, the potential artifacts produced by these devices may pose as confounders for widespread clinical use of OS-CMR to accurately assess myocardial oxygenation.

4.2 Fluid Status

4.2.1 Physiological Impact

Numerous studies have been completed to assess the effects of acute hemodilution on animal and human physiology. In addition to examining physiological changes associated with hemodilution, a handful of studies have been conducted to visualize changes that occur during hemodilution utilizing magnetic resonance imaging. Understanding the underlying physiological changes is important to build understanding of results produced in MR studies.

Chapler and Cain summarized cardiac-specific physiological changes associated with isovolemic hemodilution or acute anemia from various studies using a dog model[37]. The hemodilution was usually completed by infusing 6% dextran (molecular weight between 60,000 and 75,000) in saline, while simultaneously removing arterial blood. Focusing on the cardiovascular system, one of the most prominent changes associated with hemodilution was the increased cardiac output. One of the factors explaining this rise in cardiac output is the relationship between magnitude of rise in cardiac output and reduction in blood viscosity[38]. A decrease in viscosity leads to a reduced cardiac afterload and increasing venous return[39,40]. Hatcher et al. (1959) showed that sympathectomy led to a reduced cardiac output response following rapid hemodilution. Similarly, in conscious dogs with denervated hearts, a smaller rise in cardiac output was seen following hemodilution when compared with control animals with intact innervation[41].

Another, potential explanation for increased cardiac output was related to changes in venomotor tone[42]. Chapler et al. noted a shift of blood volume from peripheral to central following hemodilution, by assessing weight changes in the dog hind-limbs[43]. The hypothesis was that the shift in blood volume would increase venous return and thus cardiac output. It was postulated that the volume shift was driven by alpha-adrenergic-mediated increase in venomotor tone. Blocking alpha-adrenergic receptors led to a reduced cardiac output response. Utilizing previously known information about aortic chemoreceptor stimulation in causing various peripheral circulatory effect, including veno-constriction, Szlyk et al. carried out another study, where aortic chemoreceptors were surgically denervated[44]. The major finding was that hemodilution-driven cardiac output response was reduced by 50% in the denervated group when compared to control animals. The last item discussed in

Chapler and Cain's review paper is redistribution of blood flow to meet increased oxygen demands as a result of anemia caused by hemodilution. Race et al. conducted a study with progressive hemodilution in anesthetized dogs until hematocrit was reduced to 10-20%[45]. The study noted that cardiac output increase was 100% while coronary blood flow was closer to 250% increase. Interestingly, vertebral, lower aortic and mesenteric arterial flow were also increased proportionally to the increase in cardiac output, while on the other hand, renal, hepatic, and carotid artery flows did not have a proportional increase.

4.2.2 Acute Hemodilution and MR

Combining oxygenation-sensitive MR with knowledge of physiological changes elicited by acute hemodilution, allows for understanding the impact of hemodilution and fluid status on signal intensity. This principle has been demonstrated in several neurological BOLD studies using animal models. Understanding that arterial and venous hemoglobin were major determinants of BOLD contrast, Lin et al. (1998) sought to assess how changing the factor that causes the magnetic susceptibility, hemoglobin concentration, would alter the MR signal intensity[46]. The group assessed the effect of mild and moderate acute hemodilution, resulting in hematrocrit (HCT) reductions from baseline values of approximately 25% (mild) and 37% (moderate). Their pertinent imaging parameters were: TR = 83ms; TE = 40ms; and flip angle = 40°. The results from the study showed a reduced R2* for mild hemodilution and an even greater reduction in R2* (inverse of T2*, 1/T2*) for the moderate hemodilution group. The group concluded that intravoxel concentration of deoxyhemoglobin was the main contributing factor causing changes in signal intensity. It was shown that the increase in signal intensity (or reduction in R2*) was proportional to the

decrease in HCT by hemodilution.

Levin et al. (2001) continued to build on the studies showing changes in MR signal intensity associated with acute hemodilution, by taking it one step further and assessing the BOLD fMRI activation changes as a result of hemodilution[47]. The group primarily assessed BOLD percent activation (BPA) in response to photic stimulation in 24 subjects (15 females, 9 males). All subjects had baseline blood hematocrit measured. In addition, in the 9 male subjects, BPA was measured twice; before and after rapid infusion of 1L normal saline. This subgroup study was done to assess the effect of acute hemodilution on stimulation-based BPA changes. The pertinent imaging parameters were: TR = 1000-2000 ms, TE = 40ms, flip angle = 66°. When assessing the differences in just baseline HCT (without any hemodilution) and BPA, the study showed a significant dependence of BPA on HCT. At baseline, there was also a sex-specific difference in BPA, with males showing a 20% greater BPA than women (5.8±2.1 vs. 4.6±1.1, $p<0.05$). Lastly, for the subgroup study with hemodilution using 1L rapid infusion saline, a 6% decrease in HCT was observed (44.6±3.6% vs. 42.0±2.4%, $p<0.05$). Correspondingly, there was a statistically significant 8% reduction in BPA as a result of hemodilution. The group concluded that the extent of BOLD signal changes due to activation were highly dependent on hematocrit, and in addition that these activation based signal changes were attenuated when hematocrit is lowered due to acute hemodilution with saline.

To date, no studies have been done to apply the findings from neurological BOLD studies to assess the effects of hemodilution on oxygenation-sensitive CMR. This would have significant implications for the future clinical use of OS-CMR in varied patient populations, especially those that display altered fluid status, such as patients with heart failure and/or

anemia. The study described in this manuscript was an initial attempt to quantify the effect of acute hemodilution on changes in myocardial signal intensity within healthy human volunteers using a 3T MRI system. The goal of the study was to assess hemoglobin concentration as a potential confounder in OS-CMR. This was completed by first assessing, in vitro, the effect of serial blood dilutions on signal intensity in a 3T environment, followed by an in vivo study.

4.3 Acquisition Parameters

Another potential confounding factor for clinical implementation of OS-CMR is the lack of standardization of MR parameters. The body of research is still relatively young and rapidly growing in OS-CMR, thus there will be need in the near future to create a standardized protocol with specified parameters in order to easily compare research and results generated by the use of this sequence.

The first issue to assess magnetic field strength. Although most recent publications in OS-CMR/BOLD-CMR have been completed using a 3T MRI system, it is worth noting that previous studies have elucidated the large difference in oxygen sensitivity when comparing both 1.5T and 3T. The major contributing factor is that T2* relaxation is reduced when going from 1.5T to 3T by a factor of 2[48]. The significance of this reduction in T2* time at a higher field strength is that oxygenation sensitive effect is increased. Dharmakumar et al., using a canine model, found a three-fold increase in oxygen sensitivity at 3T compared to 1.5T using identical sequence parameters[49]. Given the fact that 3T imaging provides increased oxygen sensitivity, the comparison of MR sequence parameters as a potential confounding factor will be limited to studies done using a 3T MRI system.

4.3.1 Echo Time (TE), Repetition Time (TR), Flip Angle (FA)

Table 1 outlines several studies completed in the last few years using oxygenation-sensitive imaging at 3T, the sequence parameters used in each study are also outlined.

Table 1: Sequence details and parameters of clinical studies using oxygenation-sensitive CMR at 3T

Author	Year	Sequence	Model	TR (ms)	TE (ms)	Flip Angle (α)
Dharmakumar et al.[49]	2008	T2-prepared SSFP	Canine	5.20	2.60	60
Jahnke et al.[17]	2009	3D T2-prepared segmented GE	CAD Patients	2.00	1.50	30
Karamitsos et al.[50]	2010	T2-prepared SSFP	CAD Patients/ Healthy Volunteers	2.86	1.43	44
Arnold et al.[19]	2012	T2-prepared SSFP	CAD Patients/ Healthy Volunteers	2.86	1.43	44
Karamitsos et al.[51]	2012	T2-prepared SSFP	Syndrome X Patients/ Healthy Volunteers	2.86	1.43	44
Karamitsos et al.[52]	2013	T2-prepared SSFP	HCM/Athletes /Healthy Volunteers	2.86	1.43	44
Fischer et al.[29]	2014	bSSFP	Healthy Volunteers	3.40	1.70	35

It can be deduced from Table 1 that currently there is no standardized protocol for optimized OS-CMR image acquisition. Gradient echo (GRE) sequences can be made more sensitive to T2* decay by adjusting echo time (TE), repetition time (TR) and flip angle[53]. Generally, increasing TE increases the T2* sensitivity of a GRE sequence. Additionally, keeping the flip angle low allows the magnetization in the longitudinal vector to remain close to fully relaxed. This also reduces T1 effects, making T2* effects more dominant[54]. Lastly,

increasing TR also reduces the T1 effects. Unfortunately, bSSFP sequences are more prone to banding artifacts when longer TRs are employed. Dharmakumer et al. tested the effects of a short TR (3.5ms) and long TR (6.0ms) SSFP BOLD imaging by assessing two features: (i) endocardial blur and (ii) myocardial inhomogeneity. The group found that although there was no statistically significant difference in image quality, the shorter TR (3.5ms) consistently achieved lower scores when assessing endocardial blur and myocardial inhomogeneity (scored 1-5, 1 = best and 5 = worst)[55]. Another important point to consider is that flip angle often needs to be adjusted in a 3T environment, as SAR (specific absorption rate) is often exceeded at 3T[48]. Specific absorption rate refers the amount of energy that is deposited or transferred to the object being imaged in a scanner due to use of RF excitation pulses. In order to minimize global and local rises in body temperature, patient safety guidelines and regulatory policies have established threshold values for SAR. Application of the same acquisition parameters used in a 1.5T scan results in a four-fold increase in SAR at 3T. Thus, possible solutions to minimize SAR are to decrease the flip angle or increase TR, the latter of which would result in flow artifacts and myocardial inhomogeneities as previously discussed[56].

5.0 Methods:

5.1 In vitro calibration study

The presence of various BOLD studies conducted in 3T environments with slight variations in acquisition techniques within each study warranted the use of an in vitro model for calibration. The use of an in vitro model allows for better control of confounding factors by limiting them to gain a clearer understanding of BOLD effects.

Preparation

Blood samples were acquired from eight swine utilized in a different study. Before the animals were sacrificed, 50-mL of arterial and venous blood was acquired.

Experimental Protocol

Thirteen heparinized 10-mL syringes were prepared to complete serial dilutions of the arterial and venous blood with saline. The following table outlines the targeted blood concentrations. All volumes are listed in mL.

Table 2: Blood dilution protocol for arterial and venous blood using saline

Syringe	**Arterial Blood Samples**		
	Concentration [Hct]	Volume [blood]	Volume [saline]
1 (A100)	100%	10	0
2 (A90)	90%	9	1
3 (A80)	80%	8	2
4 (A70)	70%	7	3
5 (A60)	60%	6	4
6 (A50)	50%	5	5
7	0%	0	10
	Venous Blood Samples		
	Concentration [Hct]	Volume [blood]	Volume [saline]
8 (V100)	100%	10	0
9 (V90)	90%	9	1
10 (V80)	80%	8	2
11 (V70)	70%	7	3
12 (V60)	60%	6	4
13 (V50)	50%	5	5

Once all dilutions were complete, 1-mL was transferred from each syringe to 3-mL heparinized blood gas analysis tubes. All syringes were emptied of air and capped to limit any confounding interactions of the blood with the environment. Blood gas analysis was completed using an ABL80 FLEX blood gas analyzer (Radiometer, Denmark) to acquire oxy-

and deoxyhemoglobin concentrations, hematocrit, and oxygen saturation values.

Magnetic Resonance Imaging Protocol

All 10-mL syringes were places in a test tube rack and the rack was then submersed in a water tub. The water tub was placed on the MRI table. Imaging was performed in a clinical 3-T scanner (MAGNETOM Skyra 3T; Siemens, Erlangen, Germany) using an 18-channel cardiac coil. Imaging was performed so that the B_0 axis was perpendicular to the long axis of the syringes. An oxygenation-sensitive bSSFP sequence was used with the following parameters – voxel size: 1.5x1.5x10.0 mm; slice thickness: 10.0mm; bandwidth: 1302Hz; TR: 3.49ms; TE: 1.57ms, flip angle: 35 degrees.

Image Analysis

All images were analyzed using certified software (cvi[42], Circle Imaging, Calgary, AB, Canada). Manual contour tracing was employed to acquire the signal intensity from each tube of blood.

Statistical Analysis

All variables were checked for Gaussian distribution using the D'Agostino-Pearson omnibus normality test. Student's t tests were performed to compare all signal intensity values between venous and arterial blood (unpaired/paired for those that passed normality, Mann-Whitney/Wilcoxon for those that failed normality). To test correlation between quantitative variables, Pearson correlation coefficients were determined. Linear regression was also performed on venous and arterial blood to compare hemoglobin

concentration and OS-SI.

All statistical analysis was performed using Prism 6 (GraphPad Software Inc., California, USA). All variables are presented as means ± standard error of mean.

5.2 In vivo volunteer study

Participants

We studied 22 healthy volunteer subjects over the age of 18 years with no prior known history of cardiovascular, cerebral, or respiratory disease. All participants were recruited through public advertisement. Participants were required to provide informed consent and complete questionnaire upon arrival to the hospital to ensure absence of contraindications for MRI. In addition, participants were instructed to refrain from consumption of caffeinated beverages and alcohol in the 12 h prior to MRI examination. Smoking was amongst the criteria for exclusion from the study, as well as pregnancy.

Experimental Protocol

Prior to start of MRI examination, an IV catheter (18G) was placed in the forearm for blood sampling and delivery of crystalloid solution. A 5mL blood sample was acquired following placement of IV catheter. The blood sample was assessed for hemoglobin concentration (g/L) and hematocrit (%). In addition, resting heart rate and non-invasive blood pressure measurements were recorded in a supine position. An alarm bell was provided and heart rate was monitored during the scan.

Following baseline (normovolemic) blood sampling, baseline images were acquired. (5-8 minutes) of 1L crystalloid solution (Lactated Ringer's Solution) was rapidly infused within

5-8 min with a pressure bag via the IV-line. Another 5mL blood sample was acquired after aspiration of residual Ringer's Solution in the catheter. Normovolemic imaging protocol was repeated in the hypervolemic state, but functional imaging was placed at the end of the protocol, as opposed to the beginning.

Cardiovascular Magnetic Resonance

Imaging was performed in a clinical 3-T scanner (MAGNETOM Skyra 3T; Siemens, Erlangen, Germany) using an 18-channel cardiac coil. All images were acquired during breath-holds at end-expiration. Left-ventricular (LV) function was assessed using a standard ECG-gated balanced steady-state free precession (bSSFP) sequence in six long-axis slices with LV-centred radial positioning (slice thickness: 8mm; TR: 3.26ms; TE: 1.43ms). OS-CMR images were acquired in one mid-ventricular short-axis slice using a bSSFP sequence. Shimming was always performed along with frequency scouts if required.

OS-CMR Protocol

At end-expiration of a single breath-hold (baseline) a oxygenation-sensitive cine was acquired using a retrospective ECG-gated bSSFP cine sequence (slice thickness: 10.0mm; TR: 3.49ms; TE: 1.57ms, flip angle: 35 degrees). Subjects were then asked to hyperventilate for 60 seconds at a rate of approximately 35 breaths per minute. A metronome was utilized to ensure consistency of hyperventilation for all subjects. Following hyperventilation, volunteers were asked to perform a maximal breath-hold at end-expiration, and images (using the same oxygenation-sensitive sequence as baseline, but with multiple measurements) were acquired continuously throughout the breath-hold. Volunteers used

the alarm bell to signal when they could no longer perform the breath-hold, and scanning was stopped.

Image Analysis

All images were analyzed using certified software (cvi[42], Circle Imaging, Calgary, AB, Canada). Left-ventricular function was assessed by use of manual endo- and epicardial contours at systole and diastole of the six long-axis views. For OS-CMR images, manual endo- and epicardial contour tracing was completed in an end-systolic frame. Mean and segmental myocardial signal intensity (SI) was automatically generated by the software following contour tracing. All SI values were expressed as percent change (ΔSI[%]) between two images.

$$\Delta SI\ (\%) = \frac{SI(post\ maneuver) - SI(baseline)}{SI(baseline)} * 100$$

For images acquired continuously during maximal breath-hold, the first image (taken immediately following hyperventilation) was used as the reference for calculating ΔSI[%]. Specifically, change in SI was assessed between single breath-hold baseline images at normovolemia and hypervolemia; as well, differences between end-hyperventilation, peak (max), and end-breath-hold SI changes were examined.

Statistical Analysis

All quantitative variables were checked for Gaussian distribution using the D'Agostino-Pearson omnibus normality test. Student's t tests were performed to compare all

signal intensity values between time points (unpaired/paired for those that passed normality, Mann-Whitney/Wilcoxon for those that failed normality). To test correlation between quantitative variables, Pearson correlation coefficients were determined.

All statistical analysis was performed using Prism 6 (GraphPad Software Inc., California, USA). All variables are presented as means ± standard error of mean.

6.0 Results:

6.1 Hemodilution in vitro study

6.1.1 Blood Analysis

All blood analysis values are summarized in Table 2 (Appendix - A). When comparing undiluted venous and arterial blood (V100 and A100, respectively) there was no significant difference between the signal intensity produced (246.5±25.4 vs. 410.0±98.3, respectively; $p = 0.13$). Conversely, when comparing venous and arterial blood at other dilutions (90, 80, 70, 60, and 50) the mean SI values were significantly different. Hemoglobin concentrations (g/L)(Figure 11) and hematocrit (%) were not significantly different when comparing arterial and venous blood at each serial dilution level.

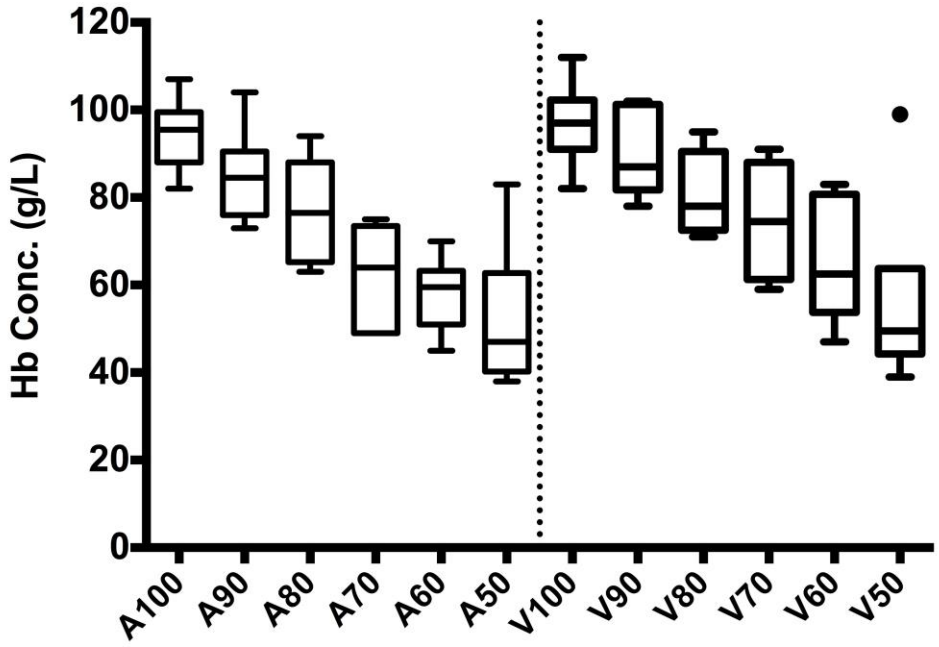

Figure 11: Tukey plot of hemoglobin concentration (g/L) for all dilutions of arterial and venous blood (V50 had an outlier point). A100 = Arterial 100% sample – no dilution, A90 = Arterial 90% sample (9mL of arterial blood and 1mL of LRS), similar dilution model followed for venous samples (V100, V90, etc.)

6.1.2 Oxygenation-Sensitive MR Correlations

A statistically significant correlation was found between %-change in SI and change in hemoglobin concentration when assessing all arterial and venous blood serial dilutions ($r = -0.6651$, $p<0.001$; $r = -0.5485$, $p<0.005$, respectively, Figure 12). Linear regression showed that slope was significantly non-zero for both arterial and venous blood.

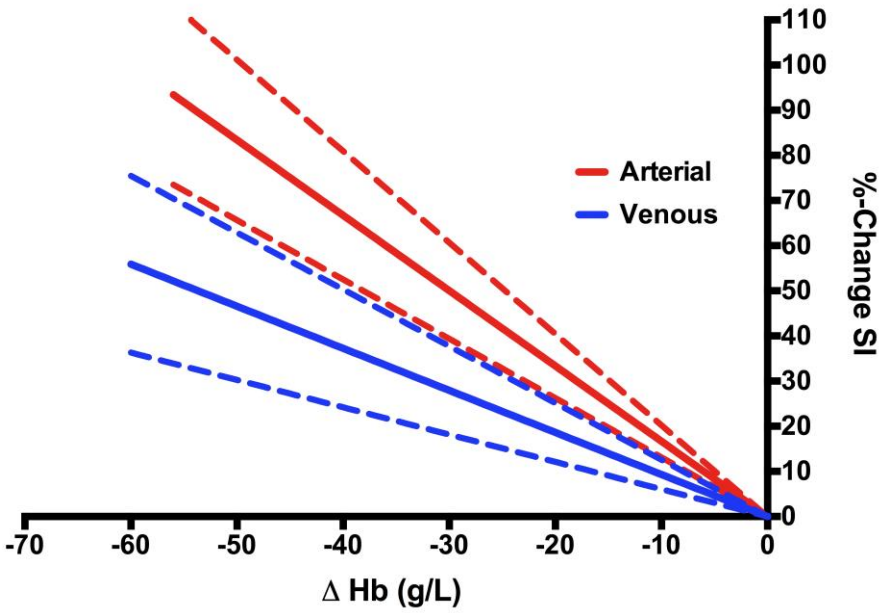

Figure 12: Linear regression analysis of arterial and venous blood %-SI change correlated to change in hemoglobin concentration (g/L)

Deoxyhemoglobin concentration (g/L) was determined using percentage deoxyhemoglobin of total hemoglobin (FHHb %) as measured by the blood gas analyzer. The change in venous blood deoxyhemoglobin concentration was significantly correlated with %-change in SI ($r = -0.6515$, $p<0.001$). In addition, venous oxygen saturation (S_vO_2) was positively correlated with %-change in SI ($r= 0.6767$, $p<0.001$).

6.2 Acute hemodilution in vivo study

6.2.1 Blood Analysis

There was a significant difference in hemoglobin concentration at baseline (142.8±3.2 g/L) and following acute hemodilution (129.1±3.2 g/L; $p<0.001$). Similarly, there was a significant difference in hematocrit between normovolemia (baseline) and hypervolemia (42.09±0.86 % vs. 38.25±0.84 %, $p<0.001$).

6.2.2 Volunteer Demographics

In total 24 volunteers were recruited, two volunteers were excluded due to claustrophobia and an undisclosed medical condition. Twenty-two volunteers completed the study. Eleven out of 22 (50%) volunteers were male and the other 11 were female. The mean age of all volunteers was 28.1±1.4 years (Figure 13). The average age of all male participants was 29.0±1.8 years. The average age of all female participants was 27.3±2.3 years. There was no significant difference in age between male and female participants.

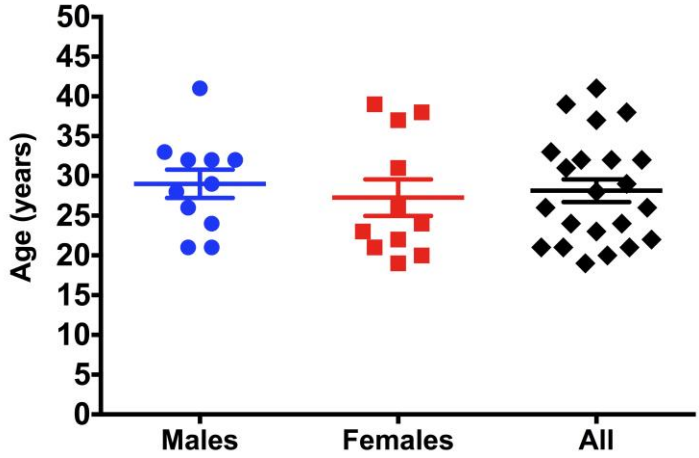

Figure 13: Age distribution of 11 male (blue), 11 female (red) and all 22 volunteers (black).

6.2.3 Cardiac function

Changes in cardiac function due to acute hemodilution with rapid infusion of 1L LRS are listed in Table 3. There was a significant increase in end-diastolic volume following hemodilution (142.5±8.0 vs. 147.3±7.9 mL, $p<0.01$). Stroke volume also displayed a significant increase following hemodilution (89.0±4.7 vs. 93.7±4.3 mL, $p<0.005$). Similarly, cardiac output had a significant increase from normovolemia to hypervolemia (5710±330 vs. 6177±323 mL/min, $p<0.005$). Interestingly, there was no significant change in heart rate, but the rate-pressure product increased significantly (8012±366 vs. 8733±345, $p<0.001$).

Table 3: Cardiac function parameters before and after acute hemodilution with 1L LRS

Cardiac Parameter	Normovolemia	Hypervolemia	p-value
End-Diastolic Volume (mL)	142.5 ± 8.0	147.3 ± 7.9	p<0.01
End-Systolic Volume (mL)	53.5 ± 4.1	53.5 ± 4.2	N.S.
Stroke Volume (mL)	89.0 ± 4.7	93.7 ± 4.3	p<0.005
Ejection Fraction (%)	63.1 ± 1.3	64.3 ± 1.3	N.S.
Cardiac Output (mL)	5710 ± 330	6177 ± 323	p<0.005
HR (beats/min)	64.3 ± 1.7	65.8 ± 1.6	N.S.
Rate-Pressure Product	8012 ± 366	8733 ± 345	p<0.001
Systolic Myocardial Mass (g)	115.8 ± 7.2	114.4 ± 6.9	N.S.

6.2.4 Baseline OS-CMR Correlations

When comparing single-breath-hold baseline images (SSFP cine) at normovolemia and hypervolemia, there was a significant difference in %-change SI (3.2±1.2%, $p<0.05$). Comparison of %-change SI and change in hemoglobin concentration showed no correlation for baseline images.

When comparing oxygenation-sensitive maps (T2*) at normovolemia and hypervolemia, there was no significant difference in T2* time (32.75±0.52 vs. 32.74±0.53 ms). Interestingly, there was a statistically significant negative correlation between T2*-time and hemoglobin concentration ($r = -0.46$, $p<0.005$).

6.2.5 Activation-dependent response

Five different time points were analyzed to assess the activation-dependent response. Once the maximal breath-hold was started and continuous imaging began, the first systolic image was analyzed to represent changes in myocardial oxygenation after hyperventilation.

During the breath-hold, four time points were analyzed: 30-sec into the breath-hold, the peak SI, average SI during plateau, and end breath-hold SI. Signal intensities assessed during the breath-hold at 30-seconds, peak, plateau, and end-BH, were all analyzed as a percent-change in SI from the SI determined at end-hyperventilation.

At normovolemia, there was a drop in SI after hyperventilation of 11.89±1.59%, decrease. At hypervolemia, there a reduction of -8.57±1.52% in SI following hyperventilation (Figure 14a). The reduction in SI following hyperventilation was significantly different ($p<0.05$) between normovolemia and hypervolemia.

There was a positive percent-change in SI (increase in SI) at the 30-second time point, which was showed a trend of being different between normovolemia and hypervolemia (11.70±1.93% vs. 8.26±1.59%, respectively; $p=0.06$; Figure 14b). The percent-change between end-hyperventilation and the peak SI reached during the breath-hold was significantly different between normovolemia and hypervolemia (14.55±1.92% vs. 11.58±1.69%, respectively; $p<0.05$; Figure 14c). Similarly, when comparing percent-change in SI from end-hyperventilation to the plateau SI during the breath-hold, there was a significant difference between the two fluid states (10.68±1.79% at normovolemia vs. 6.71±1.66% at hypervolemia; $p<0.05$; Figure 14d). Lastly, percent-change in SI calculated at the end of the maximal breath-hold was also significantly different between normovolemia and hypervolemia (6.76±1.74% vs. 2.37±1.25%, respectively; $p<0.01$; Figure 14e). Figure 15 shows the percent-change in SI observed throughout the entire breath-hold (averaged for all volunteers) at both normovolemia and hypervolemia.

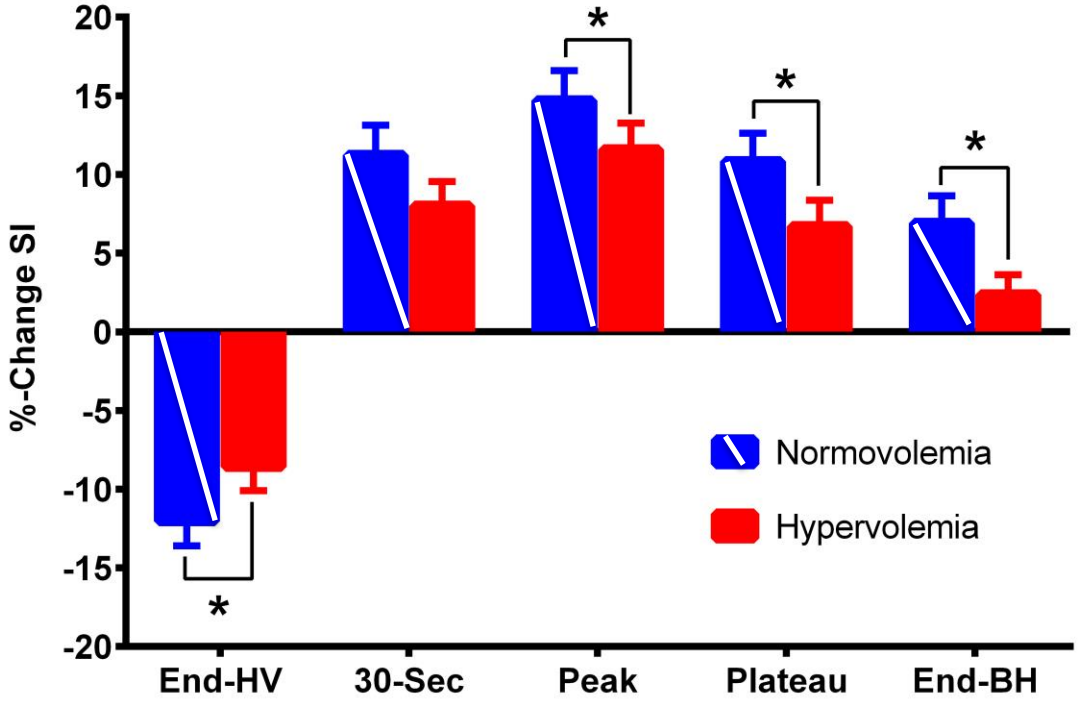

*Figure 14: A) %-change in SI from baseline following hyperventilation; B) %-change in SI from end-hyperventilation to 30-seconds into maximal voluntary breath-hold; C) %-change in SI from end-hyperventilation to peak signal intensity produced during maximal breath-hold; D) %-change in SI from end-hyperventilation to plateau (average SI of plateau period following peak SI) during breath-hold; E) %-change in SI from end-hyperventilation to end of maximal breath-hold; *p<0.05.*

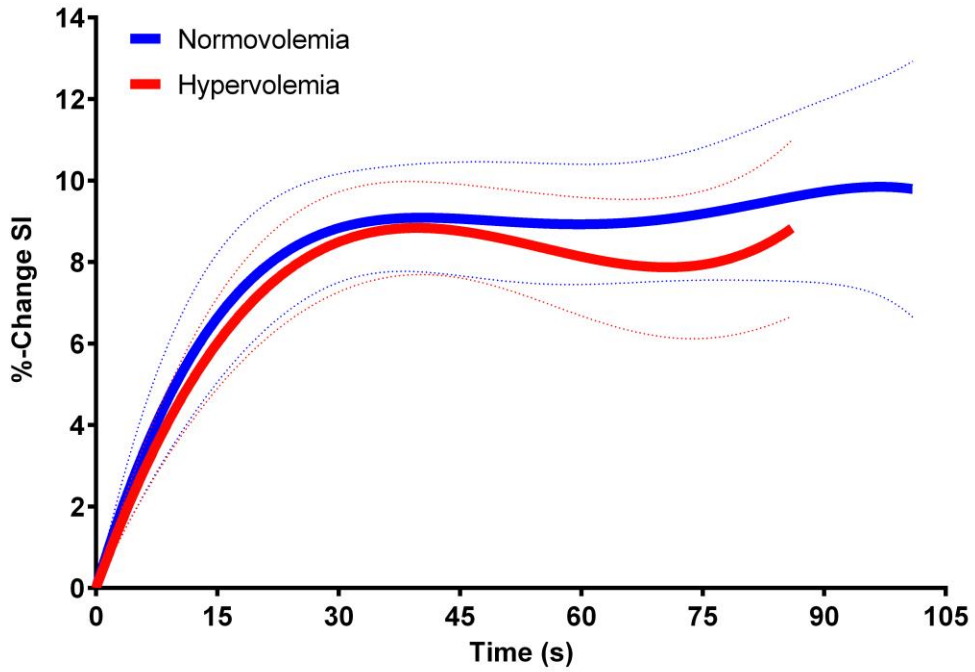

Figure 15: Non-linear regression model of %-change in SI over entire breath-hold for all volunteers at normovolemia (blue) and hypervolemia (red).

In addition, breath hold times were assessed to look at the mean time elapsed to reach peak SI, as well as total breath hold time. The mean time to reach peak SI was not significantly different between normovolemia and hypervolemia (34.15±2.73 vs. 29.99±2.46, Figure 16a). On the other hand, the total breath-hold time was significantly decreased following acute hemodilution, from 83.38±5.79 seconds to 68.66±4.76 seconds ($p<0.001$), Figure 16b.

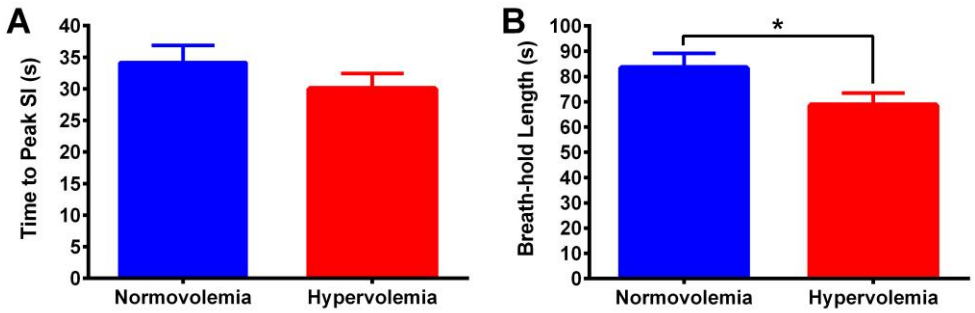

*Figure 16: A) Average time elapsed to reach peak SI during maximal voluntary breath-hold at normovolemia and hypervolemia; B) Average total length of maximal voluntary breath-hold at normovolemia and hypervolemia; *p<0.05.*

7.0 Discussion:

7.1 Fluid Status as Confounder

7.1.1 *In Vitro* Study

When assessing the porcine blood using an oxygenation-sensitive SSFP sequence, the significant correlation of both arterial and venous blood SI change to hemoglobin concentration change showed that the serial dilution led to a change in blood oxygenation and thus OS-SI. The difference in the correlation coefficient between arterial and venous blood is explained by the fact that venous blood contains deoxyhemoglobin, which acts as a perturbing agent to decrease T2* time. In arterial blood, the change in SI is largely due to dilution by saline, without any additional confounders affecting T2* time.

Previous studies, such as Lin et al. (1998) observed that the increase in SI (or reduction in R2*) following hemodilution was correlated with decrease in hematocrit, but these studies did not look at deoxyhemoglobin fraction directly. Our results highlighted a significant correlation between increase in signal intensity and decrease in deoxyhemoglobin concentration (r = -0.6515), indicative that the SSFP sequence used is

feasible to detect significant changes in SI due to hemodilution, although in vivo such severe hemodilution would not be observed. The maps showed a significant correlation between an increase in SI and decrease deoxyhemoglobin concentration, but did not show a significant correlation between decrease of total hemoglobin concentration and increase in SI. The maps are a quantitative assessment (T2* time) as opposed to the SSFP results, which are expressed as a percent change in SI compared to the undiluted V100 sample.

Direct correlation of SSFP SI and hemoglobin or deoxyhemoglobin concentration is not possible as SI values produced by an SSFP sequence is highly variable and can be affected by field inhomogeneities. This is the reason why SSFP SI values are represented as a percent-change in SI value as opposed to absolute T2* values, as this allows for comparing changes in SI during the breath-hold maneuver directly to the SI at the beginning of the maneuver. Thus this would control for any large variance due to changes in field inhomogeneities. No previous studies have assessed quantitative map data from a 3T MRI to correlate absolute T2* values with hemoglobin or deoxyhemoglobin concentrations.

The major limitation of our in vitro study was small sample size (n=5) used for assessment with the SSFP sequence. Further, only four out of the five pigs' blood samples were analyzed using maps, as one pig's data was excluded due to artifacts. A larger study would be necessary to corroborate our conclusions and correlations between decrease deoxyhemoglobin concentration and increase in T2*.

In addition, the SI generated when the imaging plane was longitudinal to the blood tubes was compared with data when the plane was transverse (Figure 17). This was done to assess any potential changes in SI that may be elicited by the orientation of the tubes, as was assessed in the study by Ogawa et al.[8]

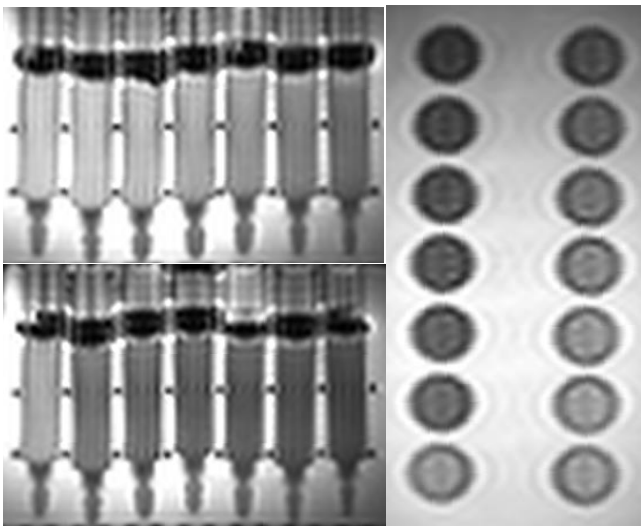

Figure 17: (Top left) arterial blood and (bottom left) venous blood imaged in a longitudinal imaging plane (perpendicular to B_0 magnetic field); (right) venous and arterial blood, respectively, imaged in a transverse plane (parallel to B_0 magnetic field).

There was no significant difference ($p = 0.243$) in SI between the longitudinal and transverse imaging protocols. This is in agreement with the findings of Ogawa et al., where blood capillary tubes were used and at much higher magnetic field strengths (7 and 8.4T){Ogawa:1990vb}-ERROR. Although, there was no significant difference between the two imaging planes, there are more noticeable artifacts present in the center of the tubes in the transverse plane, which creates a difficulty when drawing the manual contours for analysis. Artifacts were also present in the longitudinal plane, seen as dark vertical lines inside the tubes, but did not represent a significant portion of the contour volume, unlike the transverse images.

7.1.2 *In Vivo* Study

Blood analysis was the first method used to assess effective acute hemodilution following rapid infusion of 1L LRS. The significant reduction in hemoglobin (-9.6 ±2.3%) and

hematocrit (-9.1 ±2.1%) following rapid infusion indicated that acute hemodilution was effective. Among all male volunteers, the mean hemoglobin concentration at hypervolemia was 136.4 ±4.2 g/L. Among all female volunteers, the mean hemoglobin concentration at hypervolemia was 120.5 ±3.8 g/L. In comparison with laboratory reference values for adults, normal hemoglobin concentration is between 135-175 g/L for men and 120-160 g/L for women[57]. Generally, the lower limits of the aforementioned hemoglobin ranges for men and women are also used as cut-off values to indicate anemia. In the population of heart failure (HF) patients, it has been found that anywhere between 9.0% to 79.1% of patients present with anemia[58]. Although the reasons for anemia in HF patients is generally multi-faceted, one possible factor is that plasma volume expansion leads to anemia[59]. This highlights one potential patient population in which fluid status would need to be corrected for when considering oxygenation-sensitive CMR scan results.

In addition, potential factors that could have affected hemodilution and decrease in hemoglobin were assessed such as: gender, age, body mass index (BMI), and body surface area (BSA). In terms of gender, there were 11 total male volunteers (52.8%) and 10 total female volunteers (47.6%). Hemoglobin change (g/L) was compared between males and females and no significant difference was found between the groups. When comparing the age of the male versus female participants there was no significant difference and there was no correlation between age and amount of hemodilution. Body mass index, was calculated by taking mass in kilograms and dividing by the squared-height of the participant (in meters). There was no significant correlation between BMI and level amount of decrease in hemoglobin following hemodilution. It should be noted that other studies have shown that the limitation of BMI, as it is strongly influenced by age and gender, which is not taken into

account in the formula for calculatio. Body surface area was determined using the Mosteller equation[60] and showed no significant correlation with change in hemoglobin concentration following hemodilution.

Although no correlation was found between ΔSI and hemoglobin concentration when utilizing the SSFP sequence, the use of the quantitative T2* mapping sequence showed a significant negative correlation ($r=-0.4650$, $p<0.05$) between hemoglobin concentration and T2* time (ms)(Figure 18).

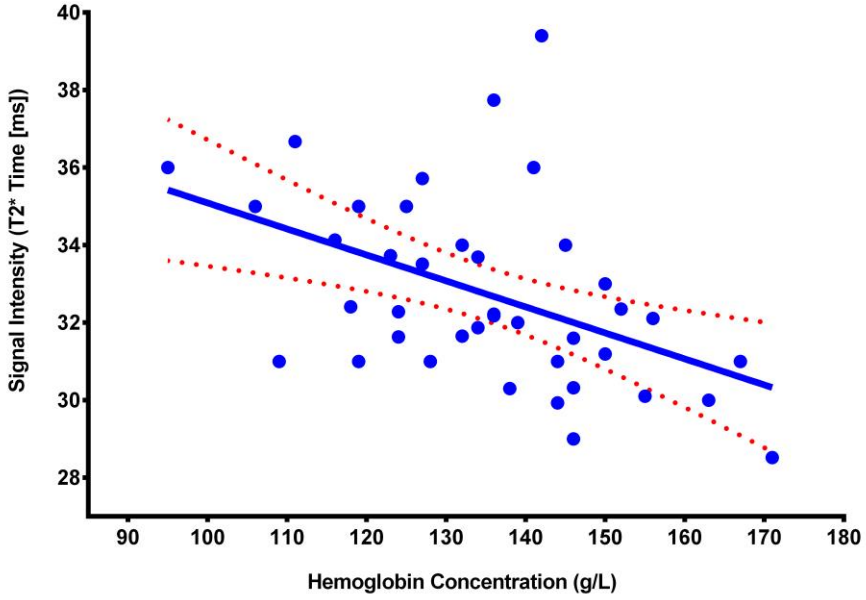

Figure 18: Negative correlation observed between T2* time (ms) of the myocardium and hemoglobin concentration (g/L) when utilizing a T2* quantitative mapping sequence.

This finding is in agreement with current understandings of susceptibility-weighted imaging, as a decrease in hemoglobin concentration (and consequently deoxyhemoglobin concentration) should result in increased T2* relaxation time. The change in T2* was not significantly different when comparing normovolemia and hypervolemia, but in a clinical setting with more severe cases of hemodilution or anemia, this change could be significant and important factor to consider in patient diagnosis. The mean T2* relaxation time at

normovolemia was 32.76 ±0.54 ms, which was slightly lower than some published values [61,62], and slightly higher than other published values at 3T[47]. This variation in results could have been due to differences in the image acquisition parameters. Although flip angle was generally similar, between 30-35 degrees, the echo train length in our sequence was 3, opposed to 8 in the other studies referenced.

In the assessment of the activation-dependent response (HVBH), it was observed that there were significant changes in OS-SI(%). At normovolemia a mean decrease of 11.68 ±1.65% from baseline was observed immediately following 60-sec of hyperventilation. This decrease following hyperventilation was similar to and even slightly larger than seen in other healthy volunteer studies[29]. The mean maximal change in SI following hyperventilation was 13.71 ±1.82%. This peak change is very similar to that seen in the Fischer, et al. study (14.8 ±6.6%)[29], following an identical breathing-maneuver protocol. The time elapsed to reach the maximal change in SI was 34.03 ±2.86 seconds, which was slightly less than that observed in the aforementioned study (40 seconds).

Five time points (end-HV, 30sec, peak, plateau, end-BH) were compared at normovolemia and hypervolemia for the assessing the change in activation-dependent response due to acute hemodilution. It was observed that at each time point there was a reduction in ΔSI (%) following acute hemodilution. At baseline, there was a 3.2±1.2% ($p<0.05$) increase in SI following hemodilution. This can be explained by the fact that a decrease in hemoglobin due rapid acute hemodilution, results in decreased concentration of deoxyhemoglobin and thus an increase in T2* relaxation time. This increase in T2* relaxation time is reflected in higher SI values obtained following hemodilution. When comparing the peak change in SI at both fluid states, it was observed that there was a significant decrease

in %-change from end-hyperventilation (14.55±1.92% at normovolemia vs. 11.58±1.69% at hypervolemia; $p<0.05$). This decrease reflects a -20.41% reduction in the peak SI change following hemodilution. In the study by Levin et al, volunteers underwent fMRI both prior to and following rapid hemodilution with 1L saline. A 6% reduction in hematocrit was observed and 8-31% reduction in BOLD percent activation (BPA). BOLD percent activation was measured in response to photic stimulation. In our study, instead of photic stimulation, breathing-maneuvers were utilized as a method to measure the activation-dependent response. The aforementioned study assessed the brain and was completed at 1.5T, therefore it is difficult to directly compare results, but our study results indicates similar changes in signal intensity with similar changes in hematocrit due to acute hemodilution.

Breath-hold capacity, assessed by measuring total breath-hold time, was significantly reduced following acute hemodilution. At normovolemia, the mean breath-hold time was 79.62 ±4.63 seconds, while at hypervolemia BH time was reduced by -16.63 ±0.62% to 66.38 ±4.39 seconds. The reduction in hemoglobin concentration following hemodilution results in a decrease in total oxygen-carrying capacity. During the voluntary apnea maneuver, chemoreceptors in the carotid arteries and brain detect carbon dioxide and oxygen levels to trigger involuntary reaction to breathe[63]. Thus, following hemodilution, the decreased oxygen levels could cause an earlier trigger to breathe.

7.2 Other Confounding Factors

Inconsistencies in image acquisition parameters remains a prominent confounding factor of future clinical use of OS-CMR. As outlined in Table 1 of recent OS-CMR studies conducted in both patients and volunteers, there is a varying range of TE, TR, and flip angles

employed. Standardization of image acquisition parameters is necessary to enable direct comparison of OS-CMR studies in the future. In addition, the use of different acquisition parameters leads to varying cut-off values for delineation of normal and abnormal results in patient populations. Clinical implementation of OS-CMR as a routine diagnostic tool will require standardization of imaging protocol and acquisition parameters to generate clear cut-off criteria.

Image quality is another potential hurdle for clinical implementation of OS-CMR. In our study, only short-axis mid-ventricular slice was acquired and assessed, resulting in adequate image quality and minimal exclusion due to artifacts. Artifacts were motion-artifacts and usually present in the first systolic image during the maximal breath-hold following hyperventilation. Nonetheless, other studies have noted that apical slices and the inferolateral segments generally have poor image quality and consequently need to be excluded from analysis[64]. This may be the reason why many clinical studies that have been completed generally limit acquisition and analysis to only the mid-ventricular slice. Although, the use of a single slice may be sufficient for proof-of-concept studies, clinical use of OS-CMR will require coverage of the entire myocardium to ensure that distal coronary disease is not overlooked.

7.3 Limitations

Several limitations for the in vitro and in vivo study require discussion. The main limitation of the in vitro experiment was the small sample size (n=6). The results showed consistency but image quality was a notable issue. The dark line artifacts throughout the test tubes presented a challenge for image analysis and signal intensity measurements. Future

in vitro studies assessing varying hemoglobin concentrations and its effect on OS-SI at 3T will require further optimization of acquisition parameters to minimize artifacts.

The in vivo assessment of hemodilution as a potential confounder of OS-CMR also has the limitation of small sample size. Sample size calculations were based on previous brain study data that displayed a mean OS-SI change of approximately 5.0±3.1% following hemodilution. In this study the mean OS-SI change at baseline was considerably lower (3.2±1.2%) following hemodilution and thus a future study with a larger sample size may lead to more significant results. One of the most important limitations of the in vivo study is the use of breathing maneuvers to assess OS-SI changes associated with the activation-dependent response. The hyperventilation and breath-hold maneuvers are highly dependent on volunteer compliance and thus cannot be entirely reliable. The use of a metronome to pace the hyperventilation rate helped to mitigate, to some degree, variations that could occur between volunteers. Unfortunately, there is no tool to ensure volunteers complete a breath-hold that is truly reflective of their maximal breath-hold capacity, thus this is entirely dependent on individual compliance. All volunteers, completed a practice HVBH maneuver prior to entering the scanner to ensure that a minimum one minute breath-hold could be comfortably completed. This was not completed in a supine position and thus the change in position once imaging began and the exposure to a novel environment and tight space of the MRI bore may have affected breath-hold capacity. For future studies, it may be beneficial to complete the breathing maneuvers twice and average the results to mitigate these issues, although in a clinical setting with patients, this may not always be feasible.

Additionally, the hemodilution itself could have caused confounding factors. The rapid hemodilution, which could mimic acute anemia and associated effects, could have

resulted in increased cardiac output and proportionate increase in coronary blood flow. This would have resulted in a higher BOLD signal intensity than would be expected if this confounding increase in cardiac output were not present.

8.0 Conclusion

The in vitro and in vivo studies completed for this project highlight the need for further studies to accurately assess potential confounding factors in the use of OS-CMR. Previous studies have shown the feasibility and improved accuracy of using non-invasive imaging such as OS-CMR as a viable alternative to other imaging modalities. Nonetheless, there is evidence, based on this study, to suggest that hemodilution or changes in hemoglobin concentration play a confounding role in the analysis and assessment of OS-SI changes. Hypervolemia leads to an increase in SI at baseline and attenuates the SI response during vasoactive breathing maneuvers. This attenuation in signal intensity would need to be accounted for and corrected in clinical assessment of OS-CMR images, especially in patient populations where changes in fluid status are prevalent, such as heart failure patients. In addition, a future study with a larger sample size, including patients, may be beneficial to derive a correction factor to correct for changes in OS-SI due to changes in hemoglobin concentration. Lastly, the clinical implementation of OS-CMR for use in varied patient populations will require standardization of acquisition parameters to ensure easy comparison of clinical studies, and consequently to create clear diagnostic criteria and guidelines for the use of OS-CMR.

9.0 References

1. World Health Organization. Global Status Report On Noncommunicable Diseases 2014. (2014).

2. Otero, H. J. *et al.* Cost-effective diagnostic cardiovascular imaging: when does it provide good value for the money? *Int. J. Cardiovasc. Imaging* **26,** 605–612 (2010).

3. Schuijf, J. D. *et al.* Cardiac imaging in coronary artery disease: differing modalities. *Heart* **91,** 1110–1117 (2005).

4. Ridgway, J. P. Cardiovascular magnetic resonance physics for clinicians: part I. *J. Cardiovasc. Magn. Reson.* **12,** 71 (2010).

5. Westbrook, C., Roth, C. K. & Talbot, J. *MRI in practice*. **4th,** (Wiley-Blackwell, 2011).

6. Ogawa, S., Lee, T. M., Nayak, A. S. & Glynn, P. Oxygenation-sensitive contrast in magnetic resonance image of rodent brain at high magnetic fields. *Magn. Reson. Med.* **14,** 68–78 (1990).

7. Dumoulin, C. L., Souza, S. P. & Hart, H. R. Rapid scan magnetic resonance angiography. *Magn. Reson. Med.* **5,** 238–245 (1987).

8. Ogawa, S., Lee, T. M., Kay, A. R. & Tank, D. W. Brain magnetic resonance imaging with contrast dependent on blood oxygenation. *Proc. Natl. Acad. Sci. U. S. A.* **87,** 9868–9872 (1990).

9. Atalay, M. K., Forder, J. R., Chacko, V. P., Kawamoto, S. & Zerhouni, E. A. Oxygenation in the rabbit myocardium: assessment with susceptibility-dependent MR imaging. *Radiology* **189,** 759–764 (1993).

10. Wendland, M. F. *et al.* Endogenous susceptibility contrast in myocardium during apnea measured using gradient recalled echo planar imaging. *Magn. Reson. Med.* **29,** 273–276 (1993).

11. Li, D., Dhawale, P., Rubin, P. J., Haacke, E. M. & Gropler, R. J. Myocardial signal response to dipyridamole and dobutamine: demonstration of the BOLD effect using a double-echo gradient-echo sequence. *Magn. Reson. Med.* **36,** 16–20 (1996).

12. McGuinness, M. E. & Talbert, R. L. Pharmacologic stress testing: experience with dipyridamole, adenosine, and dobutamine. *Am. J. Hosp. Pharm.* **51,** 325–328 (1994).

13. Shea, S. M. *et al.* T2-prepared steady-state free precession blood oxygen level-dependent MR imaging of myocardial perfusion in a dog stenosis model. *Radiology* **236,** 503–509 (2005).

14. Vöhringer, M. *et al.* Oxygenation-sensitive CMR for assessing vasodilator-induced changes of myocardial oxygenation. *J. Cardiovasc. Magn. Reson.* **12,** 20 (2010).

15. Wacker, C. M. *et al.* Susceptibility-sensitive magnetic resonance imaging detects human myocardium supplied by a stenotic coronary artery without a contrast agent. *J. Am. Coll. Cardiol.* **41,** 834–840 (2003).

16. Friedrich, M. G., Niendorf, T., Schulz-Menger, J., Gross, C. M. & Dietz, R. Blood Oxygen Level-Dependent Magnetic Resonance Imaging in Patients with Stress-Induced Angina. *Circulation* **108,** 2219–2223 (2003).

17. Manka, R. *et al.* BOLD cardiovascular magnetic resonance at 3.0 tesla in myocardial ischemia. *J. Cardiovasc. Magn. Reson.* **12,** 54 (2010).

18. Karamitsos, T. D. *et al.* Relationship between regional myocardial oxygenation and perfusion in patients with coronary artery disease: insights from cardiovascular magnetic resonance and positron emission tomography. *Circ. imaging* **3,** 32–40 (2010).

19. Arnold, J. R. *et al.* Myocardial oxygenation in coronary artery disease: insights from blood oxygen level-dependent magnetic resonance imaging at 3 tesla. *J. Am. Coll. Cardiol.* **59,** 1954–1964 (2012).

20. Walcher, T. *et al.* Myocardial perfusion reserve assessed by T2-prepared steady-state free precession blood oxygen level-dependent magnetic resonance imaging in comparison to fractional flow reserve. *Circ. Cardiovasc. Imaging* **5,** 580–586 (2012).

21. Karamitsos, T. D. *et al.* Tolerance and safety of adenosine stress perfusion cardiovascular magnetic resonance imaging in patients with severe coronary artery disease. *Int. J. Cardiovasc. Imaging* **25,** 277–283 (2009).

22. FDA Safety Announcement. FDA warns of rare but serious risk of heart attack and death with cardiac nuclear stress test drugs Lexisxan (regadenoson) and Adenoscan (ADENOSINE). *US Food Drug Adm.* 1–4 (2013).

23. Ainslie, P. N. & Poulin, M. J. Ventilatory, cerebrovascular, and cardiovascular interactions in acute hypoxia: regulation by carbon dioxide. *J. Appl. Physiol.* **97,** 149–159 (2004).

24. Kety, S. S. & Schmidt, C. F. The effects of altered arterial tensions of carbon dioxide and oxygen on cerebral blood flow and cerebral oxygen consumption of normal young men. *J. Clin. Invest.* **27,** 484–492 (1948).

25. Beaudin, a. E. *et al.* Cerebral and myocardial blood flow responses to hypercapnia and hypoxia in humans. *AJP Hear. Circ. Physiol.* **301,** H1678–H1686 (2011).

26. Case, R. B. & Greenberg, H. The response of canine coronary vascular resistance to local alterations in coronary arterial P CO2. *Circ. Res.* **39,** 558–566 (1976).

27. Guensch, D. P., Fischer, K., Flewitt, J. a. & Friedrich, M. G. Impact of Intermittent Apnea on Myocardial Tissue Oxygenation-A Study Using Oxygenation-Sensitive Cardiovascular Magnetic Resonance. *PLoS One* **8,** 1–6 (2013).

28. Guensch, D. P. *et al.* Breathing manoeuvre-dependent changes in myocardial oxygenation in healthy humans. *Eur. Heart J. Cardiovasc. Imaging* **15,** 409–414 (2014).

29. Fischer, K., Guensch, D. P. & Friedrich, M. G. Response of myocardial oxygenation to breathing manoeuvres and adenosine infusion. *Eur. Hear. J. - Cardiovasc. Imaging* **16,** 395–401 (2014).

30. Bernstein, M. a., Huston, J. & Ward, H. a. Imaging artifacts at 3.0T. *J. Magn. Reson. Imaging* **24,** 735–746 (2006).

31. Bernstein, M. Field Strength Dependence in MRI: Advantages and Artifacts at 3T. *Proc. ISMRM* (2006). at <http://afni.nimh.nih.gov/sscc/staff/rwcox/ISMRM_2006/ISMRM M-F 2006/files/WE_03.pdf>

32. Atalay, M. K., Poncelet, B. P., Kantor, H. L., Brady, T. J. & Weisskoff, R. M. Cardiac susceptibility artifacts arising from the heart-lung interface. *Magn. Reson. Med.* **45,** 341–345 (2001).

33. Nijveldt, R. *et al.* 3.0 T cardiovascular magnetic resonance in patients treated with coronary stenting for myocardial infarction: evaluation of short term safety and image quality. *Int. J. Cardiovasc. Imaging* **24,** 283–291 (2008).

34. Hargreaves, B. a. *et al.* Metal-induced artifacts in MRI. *Am. J. Roentgenol.* **197,** 547–555 (2011).

35. Levine, G. N. *et al.* Safety of magnetic resonance imaging in patients with cardiovascular devices: An American heart association scientific statement from the committee on diagnostic and interventional cardiac catheterization, council on clinical cardiology, and the council on cardiovascular radiology and intervention. *Circulation* **116,** 2878–2891 (2007).

36. Gallagher, D. *et al.* How useful is body mass index for comparison of body fatness across age, sex, and ethnic groups? *Am. J. Epidemiol.* **143,** 228–239 (1996).

37. Chapler, C. K. & Cain, S. M. The physiologic reserve in oxygen carrying capacity: studies in experimental hemodilution. *Can. J. Physiol. Pharmacol.* **64,** 7–12 (1986).

38. Fowler, N. O. & Holmes, J. C. Experimental and laboratory reports. *Am. Heart J.* **68,** 204–213 (1964).

39. Fowler, N. O. & Holmes, J. C. Blood viscosity and cardiac output in acute experimental anemia. *J. Appl. Physiol.* **39,** 453–456 (1975).

40. Murray, J. F., Escobar, E. & Rapaport, E. Effects of blood viscosity on hemodynamic responses in acute normovolemic anemia. *Am. J. Physiol.* **216,** 638–642 (1969).

41. Hatcher, J., Sadik, N. & Baumber, J. The effect of sympathectomy (Stellate T5) on cardiovascular responses to anaemia produced by dextran-for-blood exchange. *Proc Can Fed Biol Soc* **2,** (1959).

42. Guyton, A. C. *Circulatory physiology: Cardiac output and its regulation*. (W.B. Saunders Company, 1963).

43. Chapler, C. K., Stainsby, W. N. & Lillie, M. a. Peripheral vascular responses during acute anemia. *Can. J. Physiol. Pharmacol.* **59,** 102–107 (1981).

44. Szlyk, P., King, C., Jennings, D., Cain, S. & Chapler, C. The role of aortic chemoreceptors during acute anemia. *Can. J. Physiol. Pharmacol.* **62,** 519–23 (1984).

45. Race, D., Dedichen, H. & Schenk, W. J. Regional blood flow during dextran-induced normovolemic hemodilution in the dog. *J. Thorac. Cardiovasc. Surg.* **53,** 578–86 (1967).

46. Lin, W., Paczynski, R. P., Celik, A., Hsu, C. Y. & Powers, W. J. Effects of acute normovolemic hemodilution on T2*-weighted images of rat brain. *Magn. Reson. Med.* **40,** 857–864 (1998).

47. Levin, J. M. *et al.* Influence of baseline hematocrit and hemodilution on BOLD fMRI activation. *Magn. Reson. Imaging* **19,** 1055–1062 (2001).

48. Oshinski, J. N., Delfino, J. G., Sharma, P., Gharib, A. M. & Pettigrew, R. I. Cardiovascular magnetic resonance at 3.0 T: current state of the art. *J. Cardiovasc. Magn. Reson.* **12,** 55 (2010).

49. Dharmakumar, R. *et al.* Assessment of regional myocardial oxygenation changes in the presence of coronary artery stenosis with balanced SSFP imaging at 3.0T: Theory and experimental evaluation in canines. *J. Magn. Reson. Imaging* **27,** 1037–1045 (2008).

50. Karamitsos, T. D. *et al.* Relationship between regional myocardial oxygenation and perfusion in patients with coronary artery disease: insights from cardiovascular magnetic resonance and positron emission tomography. *Circ. imaging* **3,** 32–40 (2010).

51. Karamitsos, T. D. *et al.* Patients with syndrome X have normal transmural myocardial perfusion and oxygenation: A 3-T cardiovascular magnetic resonance imaging study. *Circ. Cardiovasc. Imaging* **5,** 194–200 (2012).

52. Karamitsos, T. D. *et al.* Blunted myocardial oxygenation response during vasodilator stress in patients with hypertrophic cardiomyopathy. *J. Am. Coll. Cardiol.* **61,** 1169–1176 (2013).

53. Chavhan, G. B., Babyn, P. S., Thomas, B., Shroff, M. M. & Haacke, E. M. Principles, Techniques, and Applications of T2*-based MR Imaging and Its Special Applications1. **29,** 1433–1449 (2009).

54. Nitz, W. R. & Reimer, P. Contrast mechanisms in MR imaging. *Eur. Radiol.* **9,** 1032–1046 (1999).

55. Zhou, X. *et al.* Artifact-reduced two-dimensional cine steady state free precession for myocardial blood-oxygen-level-dependent imaging. *J. Magn. Reson. Imaging* **31,** 863–871 (2010).

56. Wieben, O., Francois, C. & Reeder, S. B. Cardiac MRI of ischemic heart disease at 3 T: Potential and challenges. *Eur. J. Radiol.* **65,** 15–28 (2008).

57. Sluss, P. M., Ph, D. & Lewandrowski, K. B. Laboratory Reference Values. *N. Engl. J. Med.* **351,** 2461–2461 (2004).

58. Silverberg, D. S. *et al.* The use of subcutaneous erythropoietin and intravenous iron for the treatment of the anemia of severe, resistant congestive heart failure improves cardiac and renal function and functional cardiac class, and markedly reduces hospitalizations. *J. Am. Coll. Cardiol.* **35,** 1737–1744 (2000).

59. Tang, Y.-D. & Katz, S. D. Anemia in chronic heart failure: prevalence, etiology, clinical correlates, and treatment options. *Circulation* **113,** 2454–2461 (2006).

60. Mosteller, R. D. Simplified Calculation of Body-Surface Area. *New Engl. J. Med.* **317,** (987).

61. Zia, M. I. *et al.* Characterizing myocardial edema and hemorrhage using quantitative t2 and t2* mapping at multiple time intervals post ST-segment elevation myocardial infarction. *Circ. Cardiovasc. Imaging* **5,** 566–572 (2012).

62. Zaman, A. *et al.* Robust myocardial T2 and T2* mapping at 3T using image-based shimming. *J. Magn. Reson. Imaging* **1020,** 1013–1020 (2014).

63. Parkes, M. J. Breath-holding and its breakpoint. *Exp. Physiol.* **91,** 1–15 (2006).

64. Friedrich, M. G. & Karamitsos, T. D. Oxygenation-sensitive cardiovascular magnetic resonance. *J. Cardiovasc. Magn. Reson.* **15,** 43 (2013).

10.0 Appendices

10.1 Appendix A - Tables

Table 4: Summary of blood analysis results for in vitro study. FHHb(%): Deoxyhemoglobin amount as a percentage of total hemoglobin.

	Total Hb Conc. (g/L)	FHHb (%)	DeoxyHb Conc. (g/L)	S_vO_2 (%)
A100	92.0 ±2.8			
A90	81.0 ±2.6			
A80	75.2 ±5.5			
A70	65.0 ±4.8			
A60	60.6 ±2.7			
A50	45.8 ±3.2			
V100	93.8 ±3.1	34.7 ±4.8	32.7 ±5.1	64.3 ±4.9
V90	87.2 ±4.0	33.8 ± 3.6	29.4 ±3.2	65.2 ±3.6
V80	79.0 ± 4.3	32.7 ±4.1	25.8 ±3.3	66.2 ±4.2
V70	72.2 ±5.7	31.4 ±3.9	22.5 ±2.9	67.6 ±4.1
V60	68.8 ±5.3	29.3 ±4.4	20.9 ±4.5	69.7 ±4.5
V50	47.2 ±2.3	26.4 ±4.4	12.2 ±1.5	72.7 ±4.5

10.2 Appendix B – Documents

Volunteer Consent Form (English)

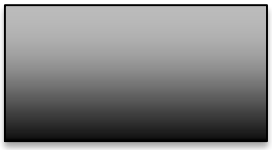

CONSENT FORM

TRIAL STUDY: ICM #13-1447

Effect of Hemodilution on Oxygenation-Sensitive Cardiovascular Magnetic Resonance Imaging

Principal investigator and collaborators

Funding: Principal investigator private funds

INFORMATION

GENERAL DESCRIPTION

You are being asked to take part in a research project as a volunteer in good health.

The study will use oxygenation-sensitive (OS) imaging to measure the oxygen in the heart muscle during a cardiac magnetic resonance imaging (MRI) exam. Our intent is to look at the change in OS-MRI signal in relation to changes in haemoglobin concentration in the blood.

This consent form describes the procedures that you must follow if you accept to participate in this study.

Before you sign this informed consent form, please take as much time as you need to read (or have read to you) and understand the information written below. Please take the opportunity to ask the study doctor or staff any questions about this research study and your rights. They will be able to provide answers to your questions.

PURPOSE OF THE STUDY

1) The Nature: This research project is aimed at developing understanding of the relationship between oxygen signal intensity changes in the heart muscle in relation to different haemoglobin concentrations in the body.

2) The Objective: To see how much the oxygen signal intensity changes in the heart when haemoglobin concentrations in the body are changed. This will be completed by increasing the fluids in the body (hemodilution).

3) Justification of the Research: The relation between signal intensity in OS-MRI and concentration of haemoglobin has been well understood in the brain. Presently, we are hoping to further our understanding of this concept in the heart, by conducting a human study. The results of this study well help in improving the diagnostic abilities of magnetic resonance imaging.

11 healthy participants will be recruited for this study, which will end in 2014. This will be a single centre study performed at the Montreal Heart Institute. The duration of volunteer participation will consist of one session of approximately 1.5 hours.

5000, rue Bélanger, Montréal (Québec) H1T 1C8 | Tél. : 514-376-3330 | Téléc. : 514-376-1355

STUDY PROCEDURE

All volunteers will receive the same exam.

Magnetic Resonance

MRI is an imaging method that uses a magnetic field with radio frequency waves, which allows doctors to see inside your body.

In the waiting room we will ask you to complete some questionnaires prior to the MRI. If a metal implant in your body may present a potential danger, you will not be allowed to participate in the study.

You will be asked to change into provided MRI clothing. An intravenous (IV) line will be placed in a vein in one arm. The IV line will be used to administer Lactated Ringer's Solution. This IV line will also be used to take 2 small blood samples during the study, each approximately 5mL (1 tablespoon). The first blood sample will be taken immediately after placing the IV line. You will be admitted to the examination room and a blood pressure cuff will be placed around your upper arm, a pulse oxymeter will be applied to your finger and 3 ECG leads on your chest. Headphones will be placed on your head, which will allow you to hear the technologist speaking to you. You can speak to the technologist by talking out loud. If at any time or for any reason you wish to stop the exam, you may do so by squeezing a rubber ball. The entire procedure will be conducted under the observation of medical staff.

We will ask you to lie on a table that will slide inside the MRI scanner. Once you are inside, the unit will emit radio frequencies that generate noise, which will be lessened by the headphones. A computer collects this information and produces multiple images. You must remain still during the exam because the movements can blur the images. We will ask you to hyperventilate and hold your breath several times during the study. You do not have to complete the breathing maneuvers if you are unable to or feel uncomfortable.

The next step will be the infusion of 1L of Lactated Ringer's Solution through the IV line that was placed at the beginning of the session. You will be asked to repeat the hyperventilation and breath holds, while a second set of images are taken. You will now be removed from the scanner and a second blood sample will be taken.

The total duration of the visit will be approximately 1.5 hours.

RISKS AND INCONVENIENCES

The MRI exam poses minimal risks if you have answered "no" to all of the contradictions on the questionnaire. There may be dangers if you have metal implants in your body. It is important to inform us if you have:

- Metal fragments in your eyes or face
- Implantations or electronic devices such as (without limitations) pacemakers, defibrillators, cochlear implants or nerve stimulators
- Surgery for cerebral blood vessels
- Claustrophobia (fear of confined spaces)
- Tattoos

The MRI machine is space confined, and if you have claustrophobic tendencies you should not participate. During the exam you can talk to the MRI technologists through a speaker system and

in an emergency you can ask to stop the exam. If you notice any heating, discomfort or a slight twitching sensation, please inform the technician so the exam may be stopped.

The breathing tests may cause slight dizziness or a mild headache. Throughout the exam, your heart rate will be monitored and if you find the side effects too strong, the breathing maneuver will be stopped immediately and the discomfort should end quickly with normal breathing. A similar study was conducted at the University of Calgary and no serious side effects occurred and no participant terminated the study.

PREGNANT WOMEN

The magnetic field used by the scanner in this study may pose a risk to developing fetuses. If you are female and suspect or know you are pregnant, you should not participate in this study. If you are a female of child-bearing age and are unsure if you are pregnant, a pregnancy test will be provided.

BENEFITS

You will not receive any direct benefit from participating in this research project. However, your participation in this project will contribute to the advancement of knowledge in cardiology. The information we get from this study will help us to improve diagnostic testing using oxygen-sensitive cardiovascular MRI.

This is not a diagnostic scan and thus cannot be used for any diagnostic purposes, neither at the time of the scan nor in the future. No liabilities can be derived. In case an incidental finding is detected which may have clinical relevance for the patient allowing for improving either longevity or quality of life, the patient will be notified by the principal investigator and a further, diagnostic work-up would be recommended.

VOLUNTARY PARTICIPATION

You are free to participate in this study or withdraw from it at any time on verbal notice without having to explain the reasons of your decision.

USE OF MY SAMPLE AND DATA FOR OTHER RESEARCH PROJECTS

You are given the opportunity to allow for your MRI data to be used only for this project, or you can allow for your MRI images and other data to be used for other additional research projects conducted by the CMR Research Centre in the future.

If you say yes, and your MRI data are to be used for another project, they will be anonymous and encoded, and will only be used after receiving the approval of the Montreal Heart Institute Research Ethics Committee. The data will be stored in the Montreal Heart Institute's research server as soon as the MRI scanner obtains the images. It will not be possible for you to remove the data from these other research projects when the data concerning you will be anonymous. Your data will be secured for 10 years to be used for further research after which they will no longer be available for other research projects.

CONFIDENTIALITY

During your participation in this study, you will be asked to fill out a relevant medical survey prior to the exam, which will be kept secure and anonymized to study number.

All data that will be collected are strictly confidential (unless of your given authorization to forward them to another party or of legal exception permitting us to communicate to them).

The research team will use your data and assess them with the data of other participants to realize this research project. To protect your identity, your personal data will be identified only by a study code that will be assigned to you instead of your name. The data concerning your identity will be kept only at the Montreal Heart Institute under the responsibility of Dr. Matthias Friedrich at the CMR Research Centre and at the Montreal Heart Institute Coordinating Centre under the responsibility of the Quality Assurance Coordinator. All research files will be stored locked and in secured files for 25 years.

For the purpose of this study, CMR images will be forwarded to the researchers of the CMR Research Centre at the MHI, and stored for up to 25 years for analysis. Prior to analysis, your data will be anonymized, identifiable only by code.

The results of this study will be published and broadcasted but no information enabling to identify you will be disclosed.

You have the right to consult and to rectify your files by contacting the principal investigator.

Should you decide to withdraw from the study the research team will cease to collect your data. The analysed data already transmitted will continue to be utilized with the data of the other participants.

Register of the Ministry

The Ministry of Health and Social Services of Quebec requires that the Montreal Heart Institute keep a registry of people who participate in research projects and this for security purposes, control of the risks, inspection and statistics. Your name and the number of your medical file will appear on this registry. You can have access at all times to this data relevant to your case to acknowledge its content and rectify it if need be.

COMPENSATION

In the event that you suffer an injury caused by the procedure or technology required by the study protocol, Dr. Friedrich of the Montréal Heart Institute will ensure that you receive all medical care that is required by your medical condition.

The CMR Research Centre at the Montréal Heart Institute does not undertake to cover the costs of these treatments and/or other costs if they are not covered by the Quebec Health Hospitalization and Insurance Plans. You will therefore assume these costs. No compensation is provided for loss of wages, invalidity or discomfort.

By signing this informed consent, you do not give up any of your legal rights. In particular, you do not release the investigator or the sponsor from their legal and professional responsibilities in case of a situation that would cause you prejudice.

INSTITUT DE CARDIOLOGIE DE MONTRÉAL

AFFILIÉE À Université de Montréal

* I C M 3 1 4 *

[redacted]

CONSENT FORM

TRIAL STUDY: ICM #13-1447

Effect of Hemodilution on Oxygenation-Sensitive Cardiovascular Magnetic Resonance Imaging

Principal investigator and collaborators

[redacted]

Funding: Principal investigator private funds

I have asked all the questions I wanted on this research project and have received appropriate answers.

I understand that I remain free to withdraw from this project at any time and this will not prejudice or change my future care.

I have read or have been read this consent form and I understand its content.

I agree for my MRI images and my other data to be used for other research projects by the CMR Research Centre after approval of the MHI Research Committee. I understand that my information will be anonymized prior to being used in another study, and as a result it will not be possible for me to remove the data from these other research projects.	I accept _____ (Partcipant's initials)	I refuse _____ (Partcipant's initials)

I, undersigned, accept to participate in this project.

Patient's signature	***Patient's Name in block letters***	***Date***	***Time***
Signature of one of the investigators	***Investigator's Name in block letters***	***Date***	***Time***

I certify that I have explained the purposes of this project to _____ and he(she) signed the consent form in my presence.

Signature of the investigator or her/his representative	***Printed Name of Investigator or her/his representative in block letters***	***Date***	***Time***

The Ethics Committee of the Research and the Development of New Technologies of the Institute of Cardiology of Montreal authorizes the beginning of recruitment on August 15th, 2014. The current version of the English consent dated from March 6th, 2014 is approved.

N.B. : The original of this form must be inserted in the patient's file, a copy kept by the investigator and a copy given to the patient.

5000, rue Bélanger, Montréal (Québec) H1T 1C8 | Tél. : 514-376-3330 | Téléc. : 514-376-1355

Volunteer Consent Form (French)

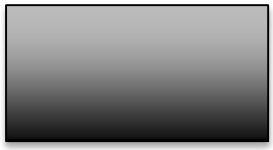

FORMULAIRE DE CONSENTEMENT

PROJET DE RECHERCHE : ICM #13-1447

Effets de l'hémodilution sur l'imagerie par résonance magnétique sensible à l'oxygénation

Investigateur principal et collaborateurs

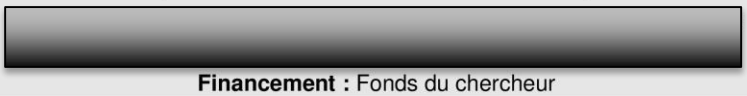

Financement : Fonds du chercheur

INFORMATION

DESCRIPTION GÉNÉRALE

Nous vous invitons à participer à un projet de recherche parce que vous êtes en bonne santé.

Cette étude utilisera une forme d'imagerie sensible à l'oxygénation (SO) afin de mesurer l'oxygénation du muscle du ventricule gauche du cœur lors d'un examen en imagerie par résonance magnétique (IRM) cardiovasculaire. Notre objectif est d'étudier les variations de signal en IRM-SO selon les changements de la concentration en hémoglobine du sang.

Ce formulaire de consentement décrit les procédures que vous devrez suivre si vous acceptez de participer à cette étude.

Avant de signer ce formulaire de consentement, veuillez prendre tout le temps nécessaire pour lire (ou vous faire lire) et comprendre l'information présentée ci-dessous. Vous pouvez consulter vos proches avant de prendre votre décision. Veuillez poser à votre médecin ou à l'équipe de recherche toutes les questions que vous avez sur la présente étude et sur vos droits. Ils devraient être en mesure de répondre à toutes vos questions.

BUT DE L'ÉTUDE

1) La nature : Ce projet de recherche vise à améliorer la compréhension de la relation entre les changements de concentration en hémoglobine et les variations correspondantes de l'intensité du signal en IRM-SO dans le muscle cardiaque.

2) L'objectif : D'observer jusqu'à quel degré l'intensité du signal en IRM-SO varie lorsque la concentration en hémoglobine du sang est manipulée par hémodilution.

3) Justification de la recherche : La relation entre l'intensité du signal en IRM-SO et la concentration en hémoglobine a fait l'objet de plusieurs études au niveau du cerveau. Présentement, nous désirons conduire une telle étude, au niveau du cœur, chez les humains. Les résultats de cette recherche pourraient servir à l'amélioration diagnostique de la résonnance magnétique.

Nous prévoyons recruter 11 volontaires en bonne santé pour cette étude qui se terminera en 2014. L'étude sera menée au Centre de recherche de l'Institut de Cardiologie de Montréal. La durée de participation pour les volontaires sera d'une session de 1,5 heure approximativement.

5000, rue Bélanger, Montréal (Québec) H1T 1C8 | Tél. : 514-376-3330 | Téléc. : 514-376-1355

DÉROULEMENT DE L'ÉTUDE

Tous les participants seront en bonne santé et subiront le même examen.

Résonance magnétique

La résonance magnétique est une méthode d'imagerie qui utilise un champ magnétique avec des ondes de radiofréquences. Elle permet aux médecins de visualiser l'intérieur du corps.

Dans la salle d'attente, nous vous demanderons de remplir un questionnaire préalable à l'examen d'IRM. Si votre corps contient une pièce de métal pouvant présenter un danger potentiel, vous ne serez pas autorisé à participer à l'étude.

Après que vous ayez revêtu la jaquette d'hôpital, un petit tube en plastique, appelé cathéter veineux, sera installé dans une veine de votre bras. Cette ligne servira à la perfusion de solution de lactate de Ringer (solution physiologique), ainsi qu'au prélèvement de deux échantillons sanguins, environ 5 mL pour chaque échantillon (1 cuillère à table). Le premier prélèvement sera fait tout de suite après l'installation du cathéter. Après que vous vous soyez allongé sur la table de l'IRM, le personnel vous installera des électrodes d'ECG sur le thorax. Un brassard de tension artérielle sera installé sur le haut de votre bras, ainsi qu'une électrode au bout d'un doigt. Des écouteurs seront placés sur vos oreilles. Durant l'examen, vous pourrez communiquer avec le technologue ou lui demander d'arrêter l'examen à tout moment. Toute la procédure sera faite en présence de technologues médicaux.

Nous vous demanderons de vous allonger sur une table qui glissera à l'intérieur de l'appareil d'IRM. Une fois que vous vous trouverez à l'intérieur, l'appareil émettra des radiofréquences qui génèrent beaucoup de bruit. Ce bruit sera atténué par des écouteurs. Un ordinateur recueille les informations et produit plusieurs images. Vous devrez demeurer immobile au cours de l'examen, car les mouvements peuvent brouiller les images. Nous vous demanderons de respirer rapidement (hyperventilation) et de retenir votre souffle à différentes périodes de temps. Vous ne serez pas obligé de compléter ces manœuvres de respiration si vous n'êtes pas capable ou si vous vous sentez inconfortable. La prochaine étape sera la perfusion de 1 litre de solution de lactate de Ringer grâce à la ligne intraveineuse. Vous devrez alors répéter les manœuvres respiratoires pendant que nous prendrons une seconde série d'images. Un deuxième échantillon de sang sera pris.

L'examen durera 1,5 heure approximativement.

RISQUES ET INCONVÉNIENTS

L'examen par résonance magnétique peut se révéler dangereux si vous avez des pièces de métal dans votre corps. Il est important de nous en informer si :

- vous avez ou avez eu des fragments de métal dans vos yeux ou votre visage ;
- vous êtes porteur de dispositifs électroniques tels que (sans s'y limiter) stimulateurs cardiaques, défibrillateurs cardiaques, implants cochléaires, ou stimulateurs nerveux ;
- vous avez eu une chirurgie des vaisseaux sanguins du cerveau ;
- vous êtes claustrophobe (peur des espaces confinés) ;
- vous avez des tatouages.

L'examen par IRM se fait dans une machine à espace restreint et les personnes claustrophobes pourraient se sentir mal à l'aise. Durant l'examen, vous pourrez parler aux technologues grâce à un système de haut-parleurs et, advenant une urgence, vous pourrez demander qu'on interrompe

l'examen. Demandez au technologue d'arrêter l'examen si vous ressentez de la chaleur, de l'inconfort ou de légers sursauts.

Lors des tests de respiration rapide ou retenue, vous pourrez ressentir que vous êtes à bout de souffle, que vous avez le souffle court, de légers étourdissements ou de légers maux de tête. Vous serez sous moniteur cardiaque pendant tout l'examen. Si les effets indésirables vous sont intolérables, nous arrêterons tout le processus et votre inconfort prendra fin rapidement lorsque vous respirerez l'air ambiant. Une étude similaire a été réalisée à l'Université de Calgary et aucun effet secondaire sérieux n'a été remarqué. Aucun participant n'a abandonné lors de ce projet.

GROSSESSE ET ALLAITEMENT

Le champ magnétique produit par le scanner peut présenter des risques pour l'enfant à naître. Si vous pensez être enceinte, vous ne devriez pas participer à l'étude. Si vous êtes une femme et que vous pensez être enceinte, vous ne devez pas participer à cette étude. Si vous êtes une femme en âge de procréer et que vous n'êtes pas certaine d'être enceinte, vous devrez passer un test de grossesse.

AVANTAGES

Vous ne retirerez aucun bénéfice direct en participant à cette étude. Toutefois, votre participation à ce projet de recherche contribuera à l'avancement des connaissances en cardiologie et à l'amélioration de l'IRM cardiovasculaire sensible à l'oxygénation comme outil diagnostique.

Ceci n'est pas un examen clinique et ne peut donc pas être utilisé à des fins de diagnostic, ni au moment de l'examen ni dans le futur. Aucune imputation ne peut en être dérivée. En cas de découverte inattendue pouvant avoir un impact clinique permettant d'améliorer la longévité ou la qualité de vie du patient, celui-ci sera avisé par l'investigateur principal et une démarche clinique pourrait être recommandée.

PARTICIPATION VOLONTAIRE

Vous êtes libre de participer à cette étude ou de vous en retirer en tout temps sur simple avis verbal sans avoir à préciser les motifs de votre décision.

UTILISATION DE MON EXAMEN ET DES DONNÉES POUR D'AUTRES PROJETS DE RECHERCHE

Nous souhaitons obtenir votre autorisation pour que votre examen d'IRM et vos données personnelles recueillies pour notre projet de recherche soient disponibles pour d'autres études menées par le Centre de Recherche en IRM cardiaque de l'Institut de Cardiologie de Montréal dans le futur.

Si vous consentez à ce que vos données soient utilisées d'autres projets de recherche, elles seront conservées et transmises de façon anonyme (anonymisées), et ce, seulement après avoir obtenu l'approbation du Comité d'Éthique de la recherche de l'Institut de Cardiologie de Montréal. Les données seront conservées dans le serveur de recherche de l'Institut de Cardiologie de Montréal à partir du moment où le système d'IRM obtient les images.

Il ne sera pas possible pour vous de vous retirer de ces autres projets de recherche lorsque les données vous concernant auront été anonymisées. Vos données seront gardées de façon sécuritaire pendant 10 ans pour des recherches plus poussées, après quoi elles ne seront plus disponibles pour d'autres projets de recherche.

CONFIDENTIALITÉ

Durant votre participation à cette étude, nous vous demanderons de remplir un questionnaire médical qui sera conservé de façon sécuritaire et sera identifié par un numéro de code.

Tous les renseignements obtenus seront strictement confidentiels (à moins d'une autorisation de votre part à les communiquer à d'autres personnes ou d'une exception de la loi nous autorisant à les communiquer).

L'équipe de recherche utilisera vos données et les analysera avec les données des autres participants pour réaliser ce projet de recherche. Pour protéger votre identité, vos données personnelles ne seront identifiées que par un code qui vous sera assigné en remplacement de votre nom. Les données révélant votre identité sont conservées à l'ICM sous la responsabilité du Dr. Matthias Friedrich. Tous les dossiers de recherche seront conservés sous clé et dans des fichiers sécurisés pendant 25 ans.

Les images obtenues seront acheminées au laboratoire de recherche du Dr. Friedrich à l'Institut de Cardiologie de Montréal et conservées pendant 25 ans.

Les résultats de cette étude seront publiés et diffusés, mais aucune information permettant de vous identifier ne sera alors dévoilée.

Si vous décidez de vous retirer de l'étude et que l'équipe cesse la collecte des données, les données déjà recueillies seront utilisées avec celles des autres participants.

Registre du ministère

Le Ministère de la Santé et des Services sociaux du Québec exige que l'Institut de Cardiologie de Montréal tienne un registre des personnes qui participent à des projets de recherche aux fins de sécurité, de contrôle des risques, d'inspection et de statistiques. Votre nom et votre numéro de dossier médical figureront dans ce registre. Vous pouvez accéder en tout temps aux données qui vous concernent pour en connaître le contenu et le faire rectifier au besoin.

COMPENSATION

Dans l'éventualité où vous seriez victime d'un préjudice causé par la procédure ou technologie requise par le protocole de recherche, le Dr Matthias Friedrich de l'ICM veillera à ce que vous receviez tous les soins que nécessite votre état de santé.

Si votre participation engendrait d'autres coûts qui ne sont pas présentement assurés par les régimes d'assurance-hospitalisation et d'assurance-maladie du Québec, ceux-ci ne sont pas couverts. Vous devrez donc en débourser les frais. De plus, aucune compensation pour perte de revenus, invalidité ou inconfort n'est prévue.

Toutefois, en signant ce formulaire de consentement, vous ne renoncez à aucun de vos droits. Notamment, vous ne libérez pas l'investigateur de ses responsabilités légales et professionnelles advenant une situation qui vous causerait préjudice.

INSTITUT DE CARDIOLOGIE DE MONTRÉAL

AFFILIÉE À Université de Montréal

* I C M 3 1 4 *

[redacted]

FORMULAIRE DE CONSENTEMENT

PROJET DE RECHERCHE : ICM #13-1447

Effets de l'hémodilution sur l'imagerie par résonance magnétique sensible à l'oxygénation

Investigateur principal et collaborateurs

[redacted]

Financement : Fonds du chercheur

J'ai eu l'occasion de poser toutes les questions voulues au sujet de ce projet et on y a répondu à ma satisfaction.

Je comprends que je demeure libre de me retirer de ce projet en tout temps sans que cela n'affecte en aucune façon les soins dont je pourrais bénéficier à l'avenir.

J'ai lu ou l'on m'a lu ce formulaire de consentement et j'en comprends le contenu.

Je suis d'accord à ce que mon examen d'IRM et mes données personnelles recueillies pour ce projet de recherche soient disponibles pour d'autres études menées par le Centre de Recherche en IRM cardiaque de l'Institut de Cardiologie de Montréal dans le futur. Ces données seront conservées et transmises de façon anonyme, et ce, seulement après avoir reçu l'approbation du Comité d'Éthique de la recherche de l'ICM. Il ne sera pas possible pour moi de me retirer de ces autres projets de recherche lorsque les données me concernant auront été anonymisées.	J'accepte _____ (Initiales du participant)	Je refuse _____ (Initiales du participant)

Je, soussigné(e), accepte de participer au présent projet de recherche.

Signature du patient	***Nom du patient en lettres moulées***	***Date (a/m/j)***	***Heure***
Signature de l'un des chercheurs	***Nom du chercheur en lettres moulées***	***Date (a/m/j)***	***Heure***

Je certifie que j'ai expliqué les buts du projet à _____et il(elle) a signé le consentement en ma présence.

Signature du chercheur ou de son délégué	***Nom du chercheur ou de son délégué en lettres moulées***	***Date (a/m/j)***	***Heure***

Le Comité d'éthique de la recherche et du développement des nouvelles technologies de l'Institut de Cardiologie de Montréal autorise le début du recrutement en date du 15 août 2013. La version courante no. 4 du consentement en français datée du 6 mars 2014 est approuvée.

N.B. : L'original de ce formulaire doit être inséré au dossier du patient, une copie gardée par l'investigateur et une copie remise au patient.

5000, rue Bélanger, Montréal (Québec) H1T 1C8 | Tél. : 514-376-3330 | Téléc. : 514-376-1355